

## Exploration significance of the Hiltaba Suite, South Australia

Anthony Budd<sup>1</sup>, Lesley Wyborn<sup>1</sup>, & Irina Bastrakova<sup>1</sup>

The recently completed 'Metallogenic potential of Australian Proterozoic granites' project highlighted the 1590-Ma Hiltaba Suite and Gawler Range

Volcanics (GRV) in the Gawler Craton as having high potential for further substantial mineral finds. This extensive magmatic entity comprises two

(geochemical) types with apparently different mineralisation associations (Fig. 1). The strongly oxidised (hematite-magnetite) and fractionated

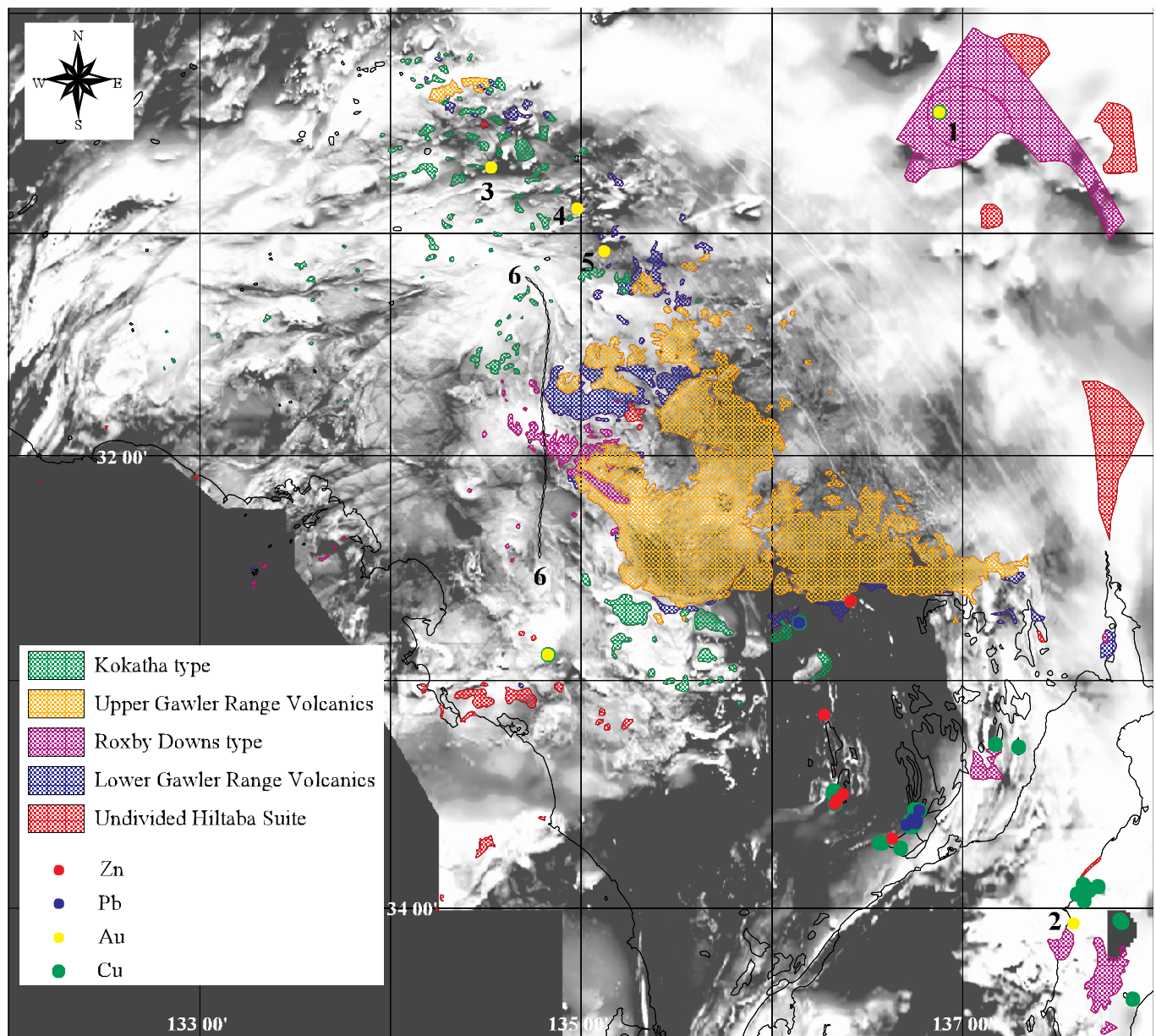


Fig. 1. Distribution of the Hiltaba Suite types and associated mineral deposits in the Gawler Craton overlain on an image derived from AGSO's 'Australian national aeromagnetic' dataset: 1, Olympic Dam Cu-Au; 2, Moonta-Wallaroo Cu-Au; 3, Tarcoola Au; 4, Earea Dam Au; 5, Glenloth Au; 6: Yarbrinda Shear Zone Au prospects. Mineral locations from the AGSO/BRS MINLOC database.

**Roxby Downs type is related to Fe-oxide–Cu–Au deposits (including the giant Olympic Dam deposit). The Kokatha type is less oxidised (ilmenite–titanomagnetite) and fractionated, and is associated with vein-hosted Au ( $\pm$  Sn  $\pm$  Ag) deposits such as Earea Dam, Glenloth, and Tarcoola. Understanding the distribution of these two magmatic types has implications for the selection of exploration models to apply to a particular area.**

### The Hiltaba volcanic–plutonic event

Volcanics and granites of the Hiltaba Suite (Drexel et al. 1993: Geological Survey of South Australia, GSSA, Bulletin 54) occur throughout the Gawler Craton, and probably extend to the Curnamona Province — including the Olary domain (Wyborn et al. 1998: in AGSO Record 1998/25, 124–129) and the Mount Painter subprovince.

The **Roxby Downs type** is composed of the following recognised granites: Moonta monzogranite (Drexel et al., 1993: op. cit.), Charleston Granite, granite at Cultana, Hiltaba Granite, Tickera Granite, Arthurton Granite, granite in the Olympic Dam area (including the Roxby Downs Granite, and Wirra

and White Dam subsuites), and granite in the Nuyts Archipelago area. The Balta and Calca Granites, for which no geochemical analyses are available, are probably also of this type. The ‘lower GRV’ (‘development’ phase of Stewart 1992: PhD thesis, University of Adelaide) is comagmatic with this type.

The Roxby Downs type includes granite (*sensu stricto*), syenogranite, quartz monzodiorite, quartz monzonite, syenite, aplite, monzogranite, and leucotonalite. Coarse-grained, porphyritic, and megacrystic varieties are common. Unlike the Kokatha type, granites of this type are commonly altered, contain hematite and magnetite, and are a distinctive brick-red colour. The Roxby Downs type is more enriched in Rb and the high-field-strength elements (HFSE) U, Th, Zr, Nb, and Ce, and more fractionated, than the Kokatha type (Fig. 2). It is mostly metaluminous, and strongly oxidised, having evolved to magmatic compositions in which hematite was the stable iron oxide. The ‘lower GRV’ is magnetite-stable (Stewart 1992: op. cit.), and ranges in composition from basalt and andesite to dacite, rhyodacite, and rhyolite with a variable silica gap between the tholeiitic basalt–andesite series and the felsic series. Felsic lithologies dominate.

The **Kokatha type** is composed of the following recognised granites: granite in the Kokatha, Tarcoola, Kingoonya, Kychering Rockhole, Minnipa, Wudinna, and Buckleboo areas. The ‘upper GRV’ (‘mature’ phase of Stewart 1992: op. cit.) is comagmatic with this type.

The Kokatha type comprises syenite, granodiorite, monzogranite, and granite (*sensu stricto*). Grainsize ranges from medium to coarse, and porphyritic textures are common. The granites are white to pink, and pyrite is a common accessory, indicating that they are more reduced than the Roxby Downs type. The type is less fractionated (lower Rb, U, Nb, and Ce at equivalent wt% SiO<sub>2</sub> are good indicators; see Fig. 2) than the Roxby Downs type, and mostly peraluminous. The ‘upper GRV’ comprises flat-lying sheets of massive porphyritic dacite and rhyodacite, crops out more extensively than the ‘lower GRV’ (much of which it probably overlies), and is ilmenite- and titanomagnetite-bearing (Stewart 1992: op. cit.).

Both suites of granites contain common accessory fluorite and apatite.

### Similarities to Curnamona Province granites

The most extensive granitoids in the Olary domain (Curnamona Province) were emplaced at ~1590 Ma, and constitute the so-called ‘regional S-type suite’ (Ashley et al. 1997: Minerals & Energy South Australia, MESA, Report Book 97/17). These rocks have considerable similarities to the Hiltaba Suite (Wyborn et al. 1998: op. cit.) both in their age and geochemical characteristics. They are probably equivalent to the Kokatha type of the Hiltaba Suite.

In the northwest Curnamona Province, granites were emplaced at ~1560 Ma in the Mount Painter and Mount Babbage inliers of the Mount Painter subprovince (Teale 1993: in GSSA Bulletin 54 (1), 149–156 & 93–100). Though younger than the Hiltaba Suite, they are similarly fractionated, mostly oxidised, I-type, fluorite-bearing, and enriched in HFSE. They are associated with occurrences of anomalous Sn, Cu, F, W, U, Y, Mo, and REE representing a variety of mineralisation styles (Teale 1993: op. cit.). However, the mineralisation’s age and relationship to the granites are poorly constrained.

### Mineralisation

The temporal and spatial association between granites of the Hiltaba Suite and

## In this issue:

|   |    |
|---|----|
| Exploration significance of the Hiltaba Suite .....   | 1  |
| Recognition, structural significance, and prospectivity of early (F <sub>1</sub> ) folds in the Minerie 1:100 000 Sheet area, Eastern Goldfields (WA) .....           | 4  |
| Phanerozoic polepath loops, and their correlation with basin development and resource accumulation .....  | 7  |
| Environmental change recorded in sediments from Tasmanian lakes ...   | 10 |
| Arid-zone groundwater recharge and palaeorecharge: insights from the radioisotope chlorine–36 .....   | 11 |
| Gamma-ray spectrometric and oxygen-isotope mapping of regional alteration halos in massive sulphide districts: an example from Panorama, central Pilbara Craton ..... | 14 |
| Subeclogitic rocks and their implications for crustal structure in the western Musgrave Block, central Australia .....  | 16 |
| A seismic model of the crust through the Broken Hill Block and Tasman Line .....  | 18 |
| Structural framework of the northeastern Yilgarn Craton and implications for hydrothermal gold mineralisation .....   | 21 |
| Towards national geoscience data standards .....  | 24 |
| Metallogenic potential of the felsic igneous rocks of the Tennant Creek and Davenport Provinces, Northern Territory .....   | 26 |

Fe-oxide–Cu–Au deposits such as Olympic Dam (Johnson & Cross 1995: Economic Geology, 90, 1046–1063), Moonta–Walleroo (Conor 1996: “The Palaeo–Mesoproterozoic geology of northern Yorke Peninsula, South Australia: Hiltaba suite-related alteration and mineralisation of the Moonta–

Walleroo Cu–Au district. Resources ’96 — field excursion 2–3 December 1996”, MESA, Adelaide), and Acropolis, Wirrda Well, Emmie Bluff, Oak Dam, and Murdie (Gow et al. 1994: Geology, 22, 633–636) has been recognised for some time. Likewise, the temporal and spatial association between Hiltaba Suite granites

and vein Au ( $\pm$  Sn  $\pm$  Ag) deposits has been demonstrated by work at Earea Dam (Daly 1993: in GSSA Bulletin 54, 138–139), Tarcoola (Daly 1993: op. cit.), Glenloth (Daly 1993: op. cit.), along with recent discoveries on the Yarbrinda Shear Zone (Martin 1996: in “Resources ’96 Convention, Adelaide, 4–5 December

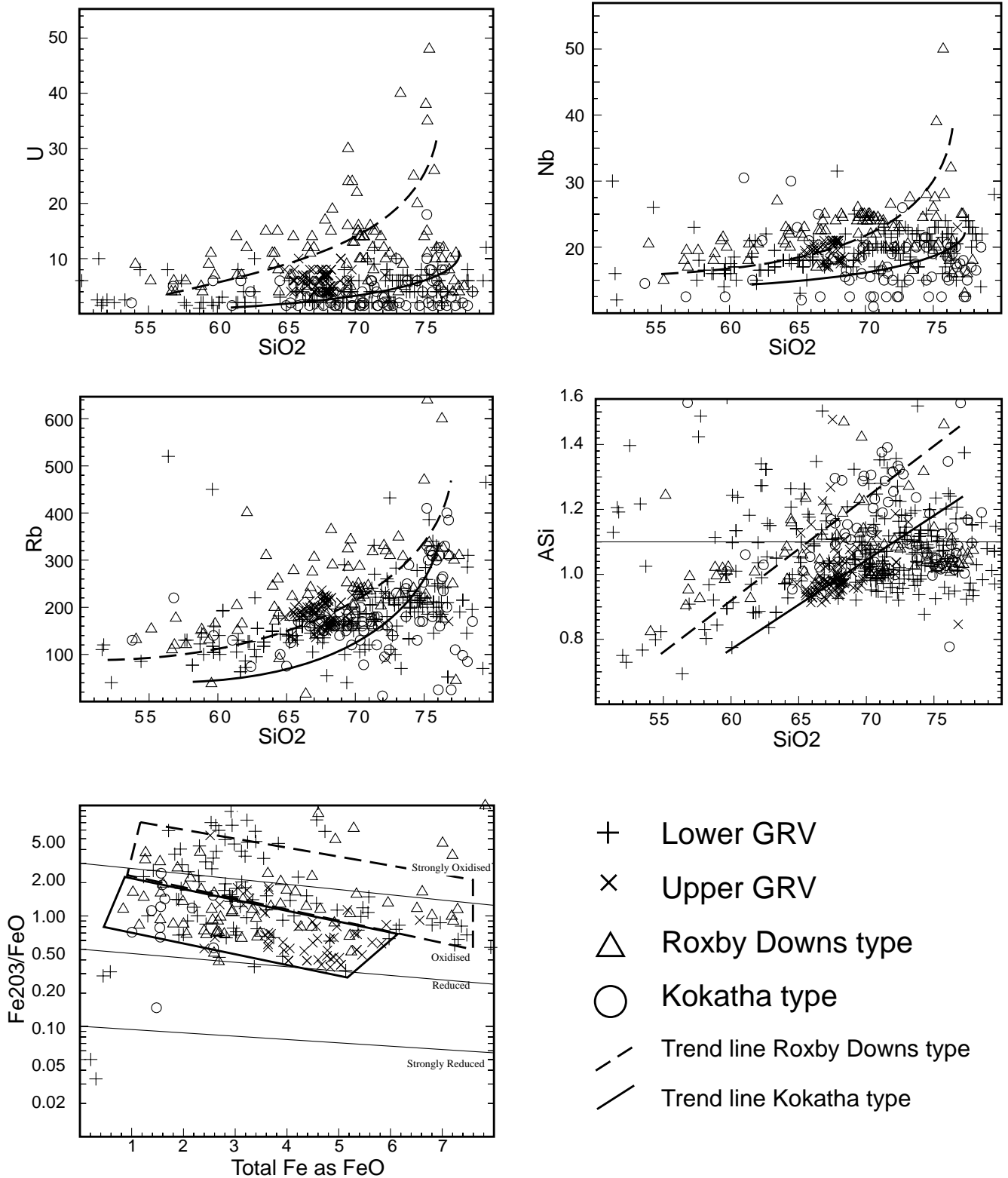


Fig. 2. Geochemical variation diagrams discriminating between the two geochemical types in the Hiltaba Suite.

1996, Abstracts", MESA, Adelaide, 90–93). However, the recently completed Proterozoic granites project is the first to recognise the correlation of different styles of mineralisation with different chemical types of the Hiltaba Suite.

### Conclusions and proposed further work

The Hiltaba Suite (granites and co-magmatic volcanics) comprises two types, each correlating with a distinct mineral association. The more oxidised Roxby Downs type is associated with Fe-oxide–Cu–Au deposits; the less oxidised Kokatha type is associated with vein Au ( $\pm$  Sn  $\pm$  Ag) deposits. The project has also identified probable extensions of the Hiltaba Suite in different areas of the Curnamona Province. This information should assist the application of exploration models in these areas.

We suggest that the geochemistry, geochronology, and geological setting of these granites and their host rocks throughout the Gawler Craton and Curnamona Province should be assessed in conjunction with detailed studies of the mineralisation associated with these granites. This in turn would assist in understanding how the magma evolved and ultimately provide more robust exploration models for these areas. Such a multidisciplinary approach has been effective in the Cloncurry district (Wyborn 1998: Australian Journal of Earth Sciences, 45, 397–411) and Pine Creek Inlier (Stuart-Smith et al. 1993: AGSO Bulletin 229). Further, detailed studies of the physical rock properties of the granites, their hosts, and the associated mineral systems will provide the knowledge necessary to interpret geophysical datasets in the areas of deep cover so prevalent in all these areas.

### Acknowledgments

This paper has resulted from the joint AGSO/State and Territory 'Metallogenic potential of Australian Proterozoic granites' project sponsored by 20 companies. It reflects contributions from Sue Daly, Colin Connor, Wayne Cowley, Martin Sheard (Primary Industries & Resources, South Australia), Paul Ashley (University of New England), and Kathy Stewart (University of Adelaide), whom we thank for their assistance. Roger Skirrow (AGSO) reviewed the manuscript. The full results of the project are being compiled for release as an AGSO Record on CD-ROM.

<sup>1</sup> Minerals Division, Australian Geological Survey Organisation, GPO Box 378, Canberra, ACT 2601; tel. +61 2 6249 9574 (AB), +61 2 6249 9489 (LW), +61 2 6249 9201 (IB); fax +61 2 6249 9971; email Anthony.Budd@agso.gov.au, Lesley.Wyborn@agso.gov.au, Irina.Bastrakova@agso.gov.au.

## Recognition, structural significance, and prospectivity of early ( $F_1$ ) folds in the Minerie 1:100 000 Sheet area, Eastern Goldfields, Western Australia

*Alastair Stewart<sup>1</sup>*

**In the Eastern Goldfields, shear zones and folds near major faults have controlled gold mineralisation, so an understanding of their configuration is essential in the search for ore. It is also needed to resolve the adjacent stratigraphy, geological evolution, and prospectivity. This report documents the recognition of large  $F_1$  folds extending over 1000 km<sup>2</sup> in the southern part of the Minerie Sheet area.  $D_1$  faults associated with one of the folds may be prospective for gold, as in the neighbouring Leonora area.**

### Regional geology

The Minerie region is located in Western Australia's Yilgarn Craton (Fig. 3), and was mapped by AGSO from 1989 to 1995 as part of the National Geoscience Mapping Accord. It comprises a sequence of Archaean greenstones — metamorphosed felsic volcanic and volcanoclastic rocks, mafic flows and sills, ultramafic rock, and minor sedimentary rocks — intruded by granite\*, rare syenite, and Proterozoic mafic dykes.

\* 'Granite' includes syenogranite, monzogranite, granodiorite, and tonalite.

### Structure

In the southern part of the Minerie Sheet area, major folds ( $F_1$  and  $F_2$ ) and foliation trends ( $S_1$  and  $S_2$ ; Fig. 4) are products of  $D_1$  and  $D_2$  deformation. Two key areas are critical to the interpretation.

Firstly, in the east, a large north-northeast to northeast-trending open to close upright syncline is cut at right-angles in its hinge zone and west limb by a steep northwest-striking foliation. The foliation is assigned to  $S_2$  because it is a prominent schistosity that parallels the general direction of  $S_2$  foliation throughout the Eastern Goldfields. Hence, the syncline is  $F_1$ . A steep north-northeast-striking foliation, also in the hinge zone of the syncline, parallels the fold's axial plane, and is assigned to  $S_1$ . The recognition of this upright  $F_1$  fold raises the possibility of others being present, and three north-northeast-trending open folds in the south may be such.

Secondly, the outcrop pattern of the volcanoclastic conglomerate, sandstone, and tuff of the Welcome Well Complex and its lateral felsic volcanic equivalents to the west is strongly suggestive of an isoclinal  $F_1$  fold subsequently folded by

the  $F_2$  Benalla Anticline. The strata face north on the northern limb and south on the southern limb. The  $F_1$  fold is therefore a tight to isoclinal anticline, possibly originally recumbent. Its limbs form a south-plunging arc, and its hinge zone has been disrupted and stopped by dolerite. Hence, the original attitudes of the  $F_1$  axis and axial plane are indeterminable. Symmetrically unfolding the Benalla Anticline about its north–south axial plane causes the  $F_1$  fold to take up an east–west trend; Figure 5 shows a possible sequence of events that led to the present outcrop pattern.

A third foliation, mapped in the country rocks next to the granite body in the north, parallels the granite margin, and may have formed by shear with or without flattening during forceful emplacement.

### Discussion

The north-northeast to northeast trend of the eastern  $F_1$  fold is unusual for the Eastern Goldfields. Large  $D_1$  structures generally trend easterly where they are not reoriented by  $D_2$  (Archibald et al. 1978: Precambrian Research, 6, 103–131), or are parallel to  $D_2$  structures where they

have been reoriented (Swager & Griffin 1990: Precambrian Research, 48, 63–73; other references in Swager 1997: Precambrian Research, 83, 18). Witt (1994: Geological Survey of Western Australia, Melita 1:100 000 Explanatory Notes) recognised north-, east-, and northeast-trending large  $F_1$  folds reoriented by  $D_3$  in the northeast of the Melita Sheet area, immediately southwest of Minerie. S. Liu (AGSO, personal communication August 1998) suggests that sinistral movement along the Kilkenny Fault (Fig. 4) could have rotated originally east–west  $F_1$  folds to their present north-northeast to north-east trend during  $D_2$  and perhaps  $D_3$ .

Chen et al. (1998: Geological Society of Australia, Abstracts 49, 79; in press: Geological Survey of Western Australia, Annual Review 1997–98) and Liu & Chen (1998: *ibid.*, 278) accounted for the north-northeast-trending folds ( $F_1$  of this report) by local compression during east–west  $D_3$  transpression. The folds formed within antidualional jogs defined by sinistral strike-slip on north-northwest-striking faults. The northwest-striking  $S_2$  foliation that cuts the eastern  $F_1$  fold (Fig. 4) contradicts their interpretation.

Two layer-parallel faults on the western limb of the folded  $F_1$  anticline in the west may be  $D_1$  faults. The folded backthrust cutting the core of this fold (Fig. 5) is also  $D_1$ .  $D_1$  shears in the Leonora area carry gold (Williams et al. 1989: Australian Journal of Earth Sciences, 36, 383–403; Williams 1998: AGSO Record 1998/9), and so the interpreted  $D_1$  faults in the Minerie area may be similarly prospective. Several small gold mines are located on or near the eastern layer-parallel fault.

Fieldwork planned in connection with second-edition compilations of the Leonora and Laverton 1:250 000 geological maps will include examination of the various foliations in the Minerie region, their nature and relationships to folds, and shear near the granite contact.

**Acknowledgments**

AGSO colleagues Songfa Liu, Alan Whitaker, and David Denham reviewed and improved the manuscript.

<sup>1</sup> Minerals Division, Australian Geological Survey Organisation, GPO Box 378, Canberra, ACT 2601; tel. +61 2 6249 9666; fax +61 2 6249 9983; email Alastair.Stewart@agso.gov.au.

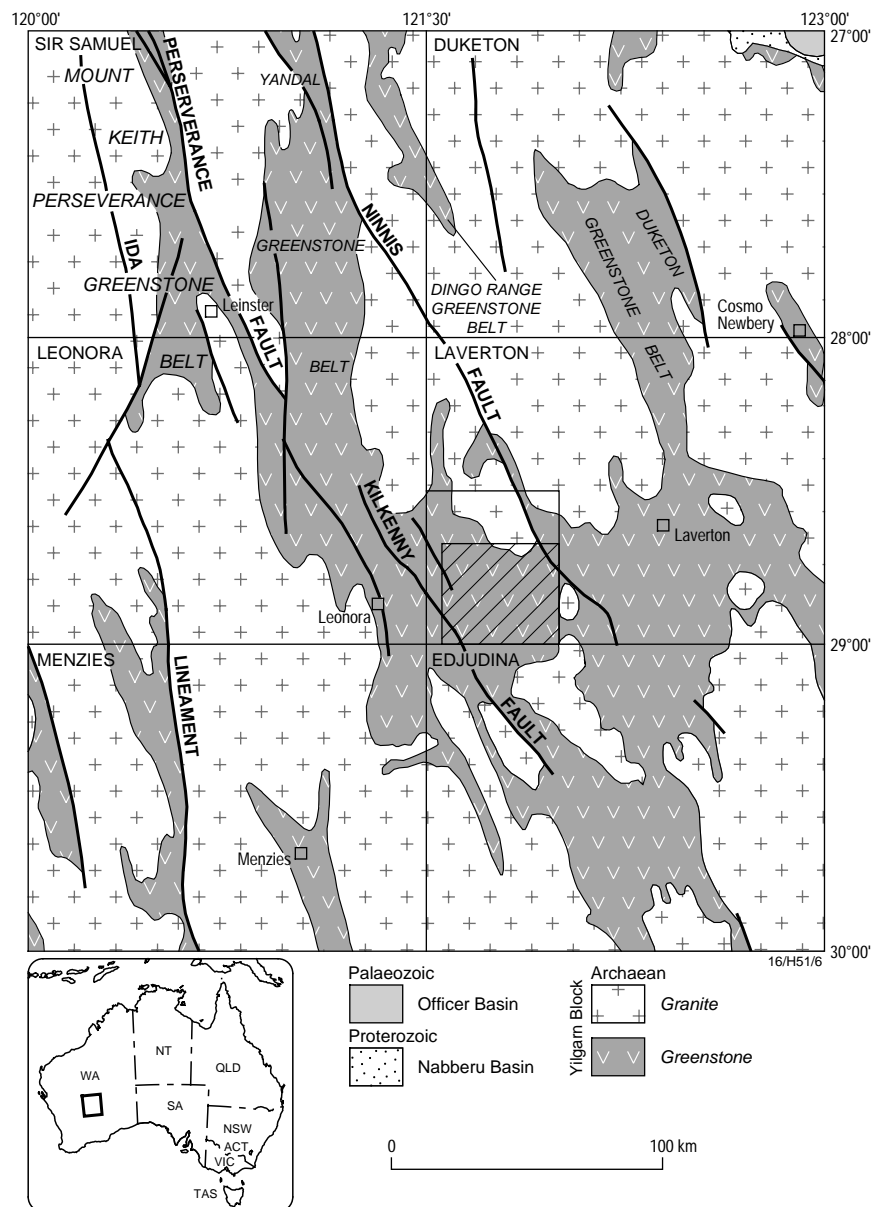
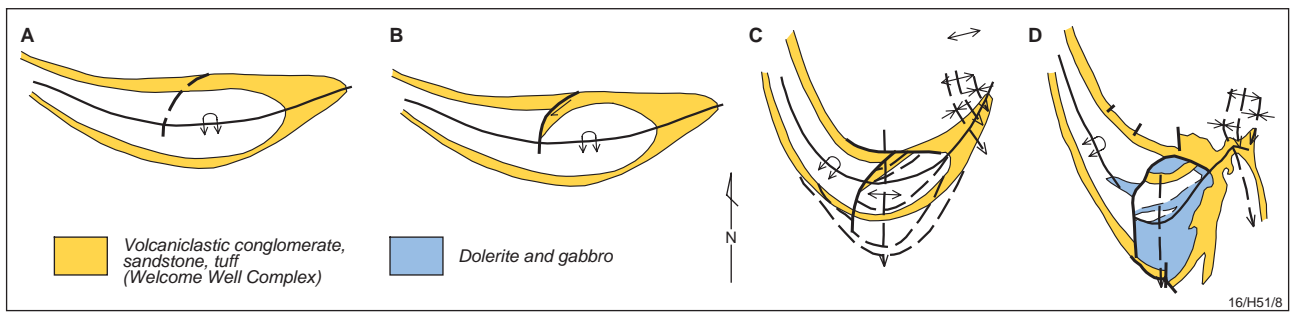
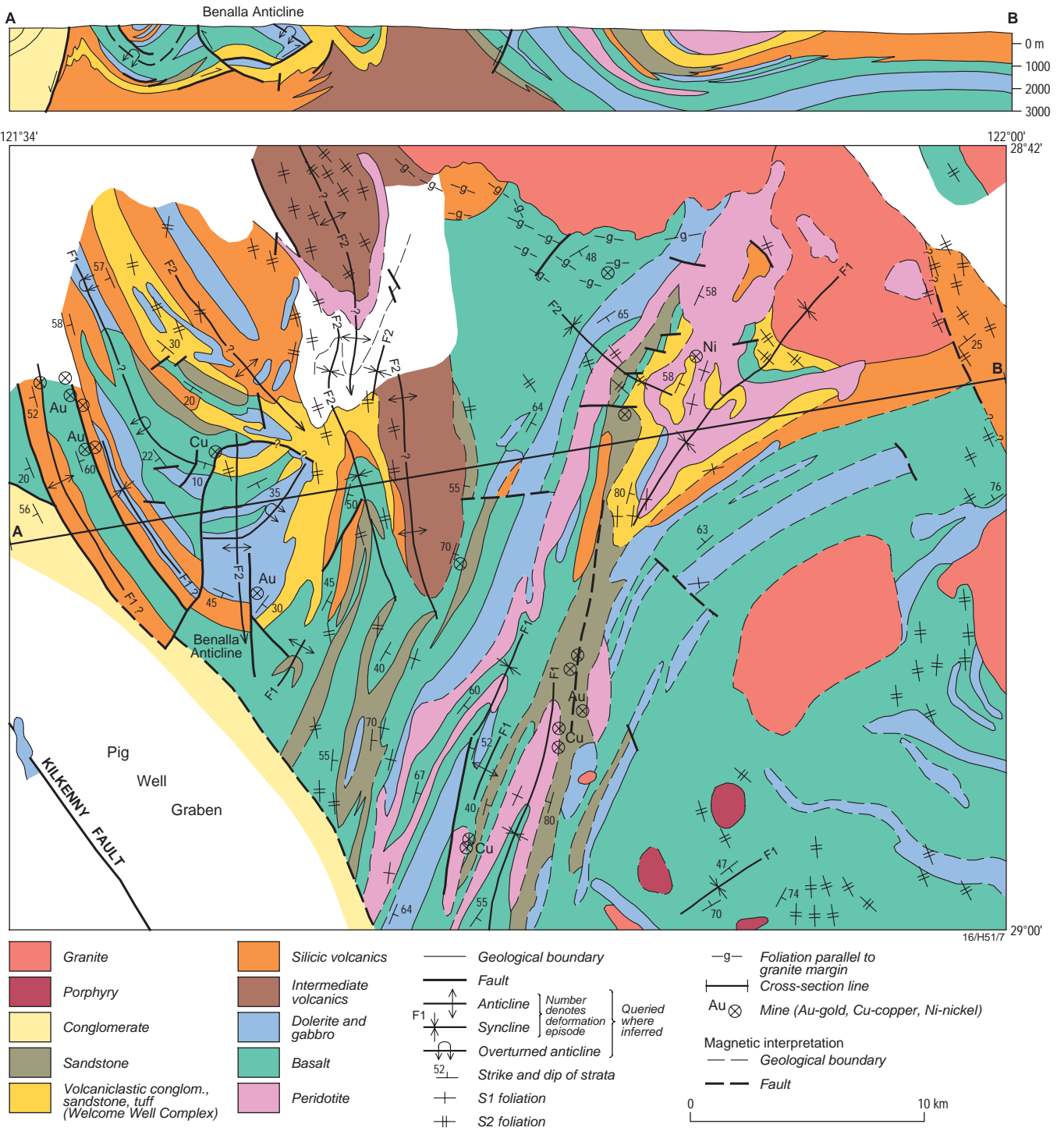


**Fig. 3. Regional geology of the central Eastern Goldfields province (after Myers & Hocking, compilers, 1988: Geological map of Western Australia, 1:2 500 000; Geological Survey of Western Australia). The rectangle represents the location of the Minerie 1:100 000 Sheet area; the hachured area, Figure 4.**

FIGURES 4 & 5 on page 6.

**Fig. 4. Solid-geology map and cross-section (from mapping by P.R.Williams, M.B.Duggan, and K.L.Currie, 1989–91, and interpretation of aeromagnetic data by the author) of the southern Minerie 1:100 000 Sheet area.**

**Fig. 5. Possible sequence of events that led to the present outcrop pattern of the Welcome Well Complex and laterally equivalent felsic volcanic units. (a) Isoclinal  $F_1$  anticline. (b) Backthrust in lower limb. (c) Flexure around  $F_2$  Benalla Anticline; dashed lines show subsequent position of strata after dolerite intrusion (which is just as likely to have occurred after stage b and before stage c). (d)  $F_2$  folding of the hinge of the  $F_1$  fold, and intrusion of dolerite.**



# Phanerozoic polepath loops, and their correlation with basin development and resource accumulation

Chris Klootwijk<sup>1</sup>

Five major loops are apparent on the Phanerozoic Australian apparent polar-wander path (polepath). They coincide with the initiation of major basin systems, indicating that a consistent and simple relationship unifies these events. Polepath loops reflect interplate movement reversals, which activate intraplate deformation and basin development. The polepath provides the only verifiable insight into Australian plate dynamics before sea-floor spreading. Its potential to detail the evolution of stress patterns and fluid-flow pathways, and thereby resource accumulation, can be realised by further detailing the loops.

Interplate movements provide the mechanism driving the intraplate deformation that leads to basin development and mineralisation (e.g., Loutit et al. 1994: in Australasian Institute of Mining & Metallurgy, Annual Conference, Darwin, 5–9 August 1994, technical program proceedings, 123–128). Seafloor-spreading data detail the movements of the Australian plate, but only as far back as the oldest break-up event recorded on the North West Shelf — Callovian–Oxfordian. Earlier movements can be traced from the polepath, but the record is less precise for latitudinal and rotational movement, and there is no control over longitudinal movement.

Australia's Palaeoproterozoic polepath has been successfully interpreted in terms of regional basin development and mineralising events (e.g., Wyborn et al. 1993: AGSO Research Newsletter, 19, 1–2; Wyborn et al. 1998: AGSO Research Newsletter, 28, 1–6; Idnurm & Wyborn 1998: AGSO Research Newsletter, 28, 6–7). The Phanerozoic polepath, however, has been less systematically explored (e.g., Klootwijk 1995: AGSO Research Newsletter, 22, 14–17; Klootwijk 1997: AGSO Research Newsletter, 26, 22–24), because attention has focused mainly on defining it. Even so, the Palaeozoic segment of the polepath is under dispute (owing to two different interpretations proposed for the middle–late Palaeozoic); the Mesozoic part is poorly defined; and the precise shape of the better established Cainozoic path has been questioned. Recent definition of the late Palaeozoic polepath for New England, however, has



Fig. 6. Australian early–middle Palaeozoic (Early Cambrian–Late Devonian) ‘spline’ polepath (see Klootwijk 1996a: op. cit., fig. 2) shown on a Gondwana reconstruction anchored to Australia in its present position.

provided new insights into links between Phanerozoic polepath features, basin development, and mineralising events (Klootwijk 1998: in AGSO Record 1998/2, 105–110).

It is now clear that the Australian Phanerozoic polepath contains five major loops (Klootwijk 1996a: in AGSO Record 1996/52; Figs. 6–8; Table 1) whose apexes coincide with the initiation of major basin systems.

These correlations link polepath loops to major basin development in a consistent but simple geodynamic relationship (though the inverse relationship does not apply universally because the polepath does not define longitudinal movements). The loops reflect interplate movement reversals; consequent intraplate deformation, mainly extensional, triggers basin development and facilitates the fluid flows that drive hydrocarbon accumulation and mineralisation.

Table 1. Australian Phanerozoic polepath loops

| Loop | Period                           | Basin initiation  |
|------|----------------------------------|---|
| L1   | Late Cambrian–Early Ordovician   | Canning Basin   |
| L2   | middle Carboniferous             | Westralian Superbasin   |
| L3   | Late Carboniferous–Early Permian | Sydney, Gunnedah, Bowen Basins; oroclinal bending S. New England  |
| L4   | Late Triassic–Early Jurassic     | Ipswich, Tarong, Clarence–Moreton, Maryborough, Surat, Eromanga Basins; rifting along New Guinea margin |
| L5   | Late Jurassic–Early Cretaceous   | Rifting along the northeastern and southern margin of the Australian plate                              |

## Loop L1: Late Cambrian–Early Ordovician

The L1 apex (Fig. 6) coincides with the Cambro–Ordovician Delamerian Orogeny and with the earliest Ordovician Sapphire Marsh Extensional Movement (Shaw et al. 1994: AGSO Record 1994/48), the onset of the Canning Basin.

## Loop L2: Middle Carboniferous

L2 on the New England polepath (Fig. 7), believed to be representative for cratonic Australia and eastern Gondwana (Klootwijk 1996a: op. cit.), indicates large-scale latitudinal movements (Klootwijk 1995: op. cit., figs. 26, 27): latest Devonian to middle Viséan northward movement over more than 30 degrees from low southern to low northern latitudes (Armidale reference), followed by late Viséan very fast southward movement to about south polar latitudes. The southward movement created an extensional regime which led to the (latest Viséan–) Namurian initiation of the Westralian Superbasin.

## Loop L3: Late Carboniferous–Early Permian

The initiation of the Sydney, Gunnedah, and Bowen Basins is fundamental to the development of the eastern Australian basins. Recent <sup>40</sup>Ar/<sup>39</sup>Ar dates narrow the onset of significant crustal extension in the (northern New England) region to ca 305 Ma (Holcombe et al. 1997: Geological Society of Australia, Special Publication 19, 66–79). This date is similar to U–Pb dates constraining the L3 apex: between 309 ± 3 Ma (Gulson et al. 1990: Australian Journal of Earth Sciences, 37, 459–469) and 297.3 ± 2.5 Ma (Black 1994: AGSO Record

1994/34) — i.e., Westphalian to Asselian on the AGSO Phanerozoic Timescale (Young & Laurie 1996: 'An Australian Phanerozoic timescale', Oxford University Press). The similarity of these dates underlines the causal relationship between plate movement reversal and extensional (less so compressional) tectonism.

The latest Carboniferous–?earliest Permian apex represents a reversal in Gondwana's rotational movement from counterclockwise in the Late Carboniferous and possibly earliest Permian to clockwise for the major part of the Permian and Triassic. These contrasting rotations greatly influenced the late Palaeozoic–early Mesozoic tectonic development of Gondwana's Laurentian and Protopacific margins. The counterclockwise rotation can be associated along the Laurentian margin with large-scale dextral shear systems in the Ural–Variscan–Mauritanides–Appalachian orogenic system (Arthaud & Matte 1977: Geological Society of America, Bulletin 88, 1305–1320) and probably also with changeover from Pangea–B (Irving 1977: Nature, 270, 304–309) to Pangea–A2 (Van der Voo & French 1974: Earth Science Reviews, 10, 99–119). Along the Protopacific margin, the rotation was associated with extensional basin development along a dextral megashear stretching from the Bowen Basin to the

Parana basin in southern South America (Visser & Praekelt 1998: Tectonophysics, 287, 201–212). The succeeding clockwise rotation of Gondwana led to compressional deformation along this zone of extensional basins — i.e., the Gondwanide Orogenies (e.g., Veevers et al. 1994: Geological Society of America, Memoir 184, 331–353), specifically the Hunter–Bowen Orogeny in eastern Australia.

The successive counterclockwise and clockwise rotations of Gondwana most likely induced dextral and sinistral displacements of New England with respect to the Lachlan–Thompson neocraton (Harrington & Korsch 1985: Australian Journal of Earth Sciences, 32, 163–179; Offler & Williams 1987: Geodynamics Series, 19, 141–151) and mega-drag-folding of the Texas, Coffs Harbour, and Manning oroclines.

**Loop L4: Late Triassic–Early Jurassic**

L4 coincides with a fundamental period in the development of the hydrocarbon-bearing basins of the North West Shelf. The loop is underdefined on the Australian Mesozoic polepath, but the better defined Indian polepath provides additional constraints within Gondwana (Klootwijk 1996a: op.cit., figs. 19, 20). The two polepaths constrain the loop's apex to between 185+ Ma (Australia) and

210–200 Ma (India).

L4 documents the reversal in eastern Gondwana's latitudinal movement from northward during the Triassic to southward during the Jurassic. By the latest Triassic, India had reached tropical latitudes; Australia's North West Shelf, about 30°S. This interplate movement reversal can be correlated with the initiation of major phases of intraplate extension, less so compression, and basin development along the eastern, northern, and northwestern margins of the Australian Gondwana fragment. The eastern margin evolved with the initiation of the Ipswich and Tarong Basins during the Late Triassic (Holcombe et al. 1997: Geological Society of Australia, Special Publication 19, 52–65) and with the probably subduction-related initiation of the Clarence–Moreton, Maryborough, Surat, and Eromanga Basins during the Early Jurassic (Williams & Korsch 1996: Geological Society of Australia, Extended Abstracts, 43, 564–568). The northern, New Guinean, margin is characterised by Late Triassic–Early Jurassic rifting (Symonds et al. 1996: Geological Society of Australia, Special Publication 43, 528–542). Elsewhere, on the North West Shelf, the interplate movement reversal can be correlated with:

- later phases of the Middle Triassic to Early Jurassic Fitzroy Movement — i.e., Late Triassic–earliest Jurassic transpressional movements fundamental to the extensive formation of reservoir and structural traps (AGSO North West Shelf Group 1994: in P.G. Purcell & R.R. Purcell (Eds.), 'The sedimentary basins of Western Australia', Petroleum Exploration Society of Australia (PESA), Perth, 63–76); and
- major Hettangian–Pliensbachian rifting accompanied by heating-enhanced source generation (Arne et al. 1989: Australian Journal of Earth Sciences, 36, 495–513).

**Loop L5: Late Jurassic–Early Cretaceous**

L5 is poorly defined on the Australian Mesozoic polepath (Fig.8) and is only marginally better so on the Indian path. The loop reflects another reversal in eastern Gondwana's latitudinal movement from southward during the Jurassic to northward during the Early Cretaceous and Cainozoic.

The latest Jurassic–earliest Cretaceous movement reversal coincides

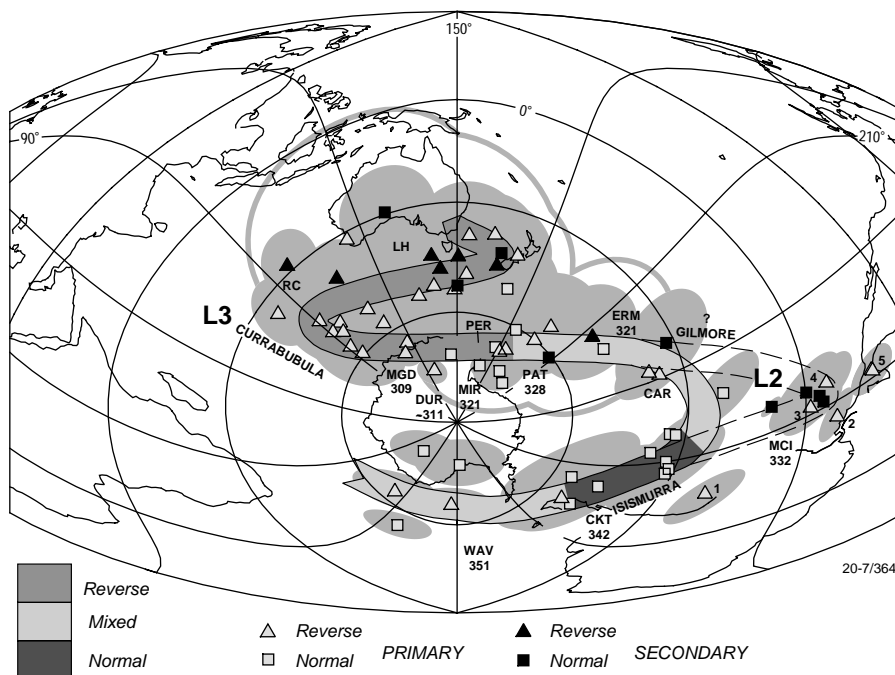


Fig. 7. Australian late Palaeozoic polepath based on Carboniferous and Permian pole positions for volcanic successions of the Tamworth Belt, New England (see Klootwijk 1996b: AGSO Record 1996/53, table 1.3, for pole position data; and Klootwijk 1996a: op. cit. for acronyms). Note that the definition of the apex of loop L2 is under review.



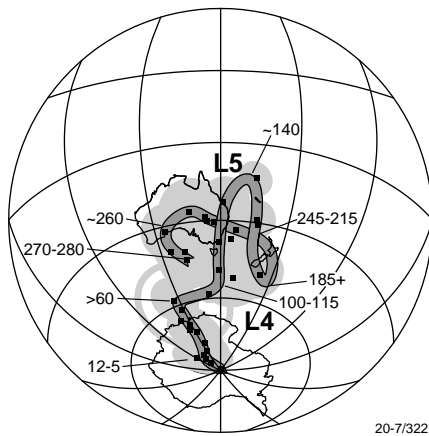


Fig. 8. Latest Palaeozoic–Cainozoic polepath for Australia.

with major rifting phases along Australia's northeastern, southern, and western margins. Along the northeastern and southern margins, the rifting is preserved in the Queensland and Townsville Troughs (Struckmeyer et al. 1994: AGSO Record 1994/50; Symonds et al. 1996: op. cit.), the Whitsunday–Proserpine–Graham Creek volcanic belt, and the Southern Rift System (e.g. Symonds et al. 1996: op. cit.). The western margin, in contrast, evinces an initial Tithonian–Berriasian compressional phase, crucial to further development of hydrocarbon traps on the North West Shelf (Etheridge & O'Brien 1994: PESA Journal, 22, 45–63), followed by (Berriasian–) Valanginian extension of the Westralian Superbasin and formation of the Gascoyne, Cuvier, and Perth Basins.

### Lesser flexures and their significance

Various smaller bends on the Phanerozoic polepath indicate directional changes, rather than reversals, in interplate movements (see Klootwijk 1996a: op. cit.). The more obvious features are:

- a Late Devonian (to possibly Early Carboniferous) broad bend coinciding with the initial phases of the Alice

- Springs Orogeny;
- two ill-defined loops of minor dimension coinciding with the Late Permian separation of Cimmerian fragments from northeastern Gondwana;
- a broad Middle–Late Triassic bend correlated with paroxysmal Hunter–Bowen tectonism;
- a latest Early Cretaceous bend preceding the opening of the Tasman Sea;
- a latest Cretaceous–earliest Tertiary bend coinciding with northward propagation of sea-floor spreading into the Capricorn and Coral Sea Basins; and
- a Mio-Pliocene excursion coinciding with the initial contact of continental Australia with the Banda Arc.

### Polepath loops, bends, and fluid movements

Several recent Australian and overseas studies have established relationships between polepath loops and bends and mineralising events. Thus, Idnurm et al. (1994: in Australasian Institute of Mining & Metallurgy, Annual Conference, Darwin, 5–9 August 1994, technical program proceedings, 53–156) correlated several inflections on the Palaeoproterozoic polepath for the McArthur Basin with mineralising events. They also linked regional magnetic overprints with pole position groupings which were close to the apexes of the inflections, and which thus could be uniquely identified and dated. Study of the temporal and spatial evolution of these magnetic overprints can provide a low-cost high-resolution facility for unravelling the evolution of fluid movement pathways, hydrocarbon accumulations, and mineral-plumbing systems.

The Phanerozoic polepath has not been explored systematically for such control on fluid movements, but its potential is evident. Its loops and bends reflect changes in movement of the

Australian plate. Attendant changes in stress regimes created and reactivated basement fracture systems, increased basement permeability, and thus focused hydrothermal flows with the potential to concentrate hydrocarbon and mineral resources. Pole positions for magnetic overprints acquired in response to fluid-flow systems are expected to lie on the younger limb and/or apex of the loops and bends.

The limited Phanerozoic-overprints data have not so far provided an analogue to the late Palaeoproterozoic association between well-grouped overprint poles and polepath kinks. Few Phanerozoic overprint groupings are directionally confined; a notable exception is the ~90–95-Ma overprints associated with the opening of the Tasman Sea. Most overprints trail polepath inflections in drawn-out suites. This may reflect ongoing remagnetisation during large-scale and fast plate movements, and may thus have the advantage of considerable resolution in the identification and dating of fluid-flow phases. Nevertheless, it is a sobering observation that, so far, only a single overprint pattern can be related to an established mineralisation phase — that is, the Early Carboniferous overprint suite recording the ~350–340-Ma mineralisation phase of the Tasman Orogenic System, which occurred after the Late Devonian (to possibly Early Carboniferous) bend (Klootwijk 1996a: op. cit., fig.5).

<sup>1</sup> Minerals Division, Australian Geological Survey Organisation and Australian Geodynamics Cooperative Research Centre, GPO Box 378, Canberra, ACT 2601; tel. +61 2 6249 9324; fax +61 2 6249 9983; email Chris.Klootwijk@agso.gov.au.

## Environmental change recorded in sediments from Tasmanian lakes

Charles E. Barton<sup>1</sup> & Eric A. Colhoun<sup>2</sup>

**Tasmania experienced a sequence of glaciations during the past few million years. Whereas many northern hemisphere lakes were scoured out by the last glaciation, which peaked at about 18–20 000 y ago, Tasmania is well supplied with lakes that lay at the fringe or beyond the limit of glaciation. Some of these lakes preserve excellent sedimentary records of environmental conditions leading to the onset of glaciation, post-glacial recovery, and the subsequent impact of fires and human occupation on the vegetation.**

Little or nothing was known about the sedimentary record in any of Tasmania's many lakes until a few years ago. Work undertaken by AGSO in collaboration mainly with the University of Newcastle (Prof. Eric Colhoun, Sharon Anker, Tony Fowler, Feli Hopf, Warwick Dyson) has established the basic characteristics of selected lakes in critical locations (Fig. 9).

Dove Lake and Lake St Clair were at the ice front and contain typical late glacial–Holocene records — namely, a basement zone of grey thixotropic glacial flour produced under late glacial conditions, overlain by organic-rich Holocene mud. Records of this type are common in northern hemisphere lakes in glaciated regions. The grey clay contains pollen that indicates the presence of herbaceous and alpine shrub vegetation communities before 11–10 000 y ago. Wet forests dominated by southern beech and *Eucalyptus* spp. developed during the Holocene.

Lake Johnston, situated a short distance below the summit of Mount Read, near Rosebery, lies in a basin containing a diverse range of plant life, including the highest-elevation growths of Huon pines yet found. One of the Huon pines here has been tree-ring-dated at 3700 y, which makes it one of the oldest trees in the world. Because of its remarkable vegetation and sensitivity to climatic change, this basin has attracted widespread interest from Quaternary scientists. Pollen analysis shows that the Huon pine has maintained a similar density for the last 10 000 y, and is a high-altitude relict species surviving from the last glaciation. The sediments preserve a record of gradual changes in direction of the geomagnetic field which can be correlated

with the dated master curve for Lake Keilambete (SW Vic.). The resulting magnetic timescale is in broad agreement with the radiocarbon ages for Lake Johnston.

Great Lake (max. depth 20 m) and Lake Echo (max. depth 23 m), at an elevation of about 850 m on the doleritic Central Plateau, and Lake Selina (max. depth 7 m), at the foot of Mount Murchison, each escaped scouring during the last glaciation. These lakes contain fascinating records of the waxing and waning of glacial conditions going back to the penultimate glaciation over 130 000 y ago. The pollen record in Lake Echo shows a sequence of shifts in *Eucalyptus* forest and alpine/steppe vegetation across the southeastern Central Plateau. The Last Glaciation Maximum was dry, and coincided with mainly herbaceous vegetation. The surface sediments in Great Lake contain evidence that eucalypt pollen is readily transported over large distances, implying that the now treeless plain on the western side of the lake reflects human impact and is not a natural feature.

Lake Selina records the Last Glacial Maximum as a prominent peak in magnetic susceptibility at 100-cm depth in a core from the deepest part of the lake (7 m). A similar peak occurs at a depth of 115 cm in a core from below 18.5 m of water in Lake Echo, 90 km to the southeast. The Lake Echo peak is considered to mark the Last Glacial Maximum. A further magnetic susceptibility high in the Lake Echo sequence is considered to mark the penultimate glacial maximum. These susceptibility peaks are attributed to intense erosion of mineral sediment in the catchments during peak glacial conditions. The pollen and vegetation record in Lake Selina is one of the best in Australia for the entire last glacial–interglacial cycle extending back to ca 130 000 y ago, and is the first Australian continental record of all the isotope substages of Zone 5 (i.e., 5a to 5e, spanning the interval 73–128 000 y ago). It shows that substages 5a, 5c, and 5e had rainforest vegetation, and that rainforest during the peak interglacial was more prominent than during the Holocene.

Macquarie Harbour was cored this

year during a project run by Paul Augustinus (University of Auckland) and David Hannan (University of Tasmania). Sediment accumulation in the Harbour is rapid, and the 6-m long sections of sulphurous brown muds recovered are thought to span no more than the late Holocene. Issues that are being addressed

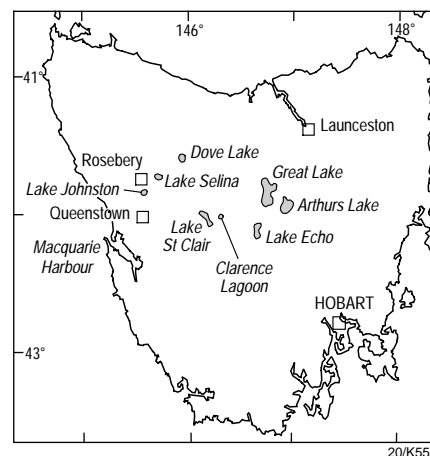


Fig. 9. Locations of the lakes in Tasmania from which sediment cores have been recovered.



Fig. 10. AGSO's Mackereth lake-bed corer surfacing in Great Lake behind Professor Eric Colhoun.

include the history of influx of mine waste into the Harbour from the Mount Lyell mine via the King River, and the acceleration of bank erosion caused by boats in the lower reaches of the Gordon River.

AGSO's Mackereth lake-bed corer was used to collect all the sediment cores. The corer is lowered to the floor of a lake, and is operated remotely from a small dingy by compressed air stored in dive bottles. Coring is accomplished by pneumatically driving 6-m-long PVC drainpipes into the sediment. On completion of coring, air is diverted into a buoyancy drum, which raises the corer to

the surface (Fig. 10). This lightweight equipment is ideal for operating in remote locations, and can be used in water depths up to 100 m. The PVC core tubes serve as permanent core retainers. Being non-magnetic, they permit rapid 'whole-core' scanning for magnetic properties such as susceptibility.

Analysis of the cores has focused mainly on the pollen content (which is diagnostic of vegetation cover),  $^{14}\text{C}$  dating (at the University of Sydney and the Australian Nuclear Science & Technology Organisation), and palaeomagnetic properties. The palaeomagnetic

properties provide stratigraphic information and, under favourable conditions, an independent timescale based on the dated master curve of geomagnetic secular variation in southeastern Australia.

<sup>1</sup> Geohazards, Land & Water Division, Australian Geological Survey Organisation, GPO Box 378, Canberra, ACT 2601; tel. +61 2 6249 9611; fax +61 2 6249 9913; email Charles.Barton@agso.gov.au.

<sup>2</sup> Department of Geology, University of Newcastle; tel. +61 2 4921 5082; fax +61 2 4921 5877; email ggeac@cc.newcastle.edu.au.

## Arid-zone groundwater recharge and palaeorecharge: insights from the radioisotope chlorine-36

Gerry Jacobson<sup>1</sup>, Richard Cresswell<sup>2</sup>, John Wischusen<sup>1</sup>, & Keith Fifield<sup>2</sup>

AGSO's collaborative 'Western water' study (*Wiluraratja kapi*; AUS.GEO News 30, October 1995, p. 9), of groundwater resources in Aboriginal lands in the southwest Northern Territory arid zone, has applied the radioisotope  $^{36}\text{Cl}$  to investigate the sustainability of community water supplies drawn from shallow aquifers in the Papunya–Kintore–Yuendumu area (Fig. 11). The  $^{36}\text{Cl}$  results have important implications for groundwater management throughout the arid zone, because substantial recharge occurs only during favourable, wet, interglacial climatic regimes. Most of the community water supplies depend on 'old' stored water.

### Location, geology, and hydrogeology of the study area

The Papunya–Kintore–Yuendumu area of 60 000 km<sup>2</sup> includes seven major Aboriginal communities and a number of outstations. It has an irregular annual rainfall of 250 mm, and annual evaporation of ~3000 mm. The Aboriginal communities are totally dependent on groundwater, which is extracted from about 200 water-bores drilled to depths of 60–200 m. Groundwater salinity, a major constraint on present and future development in this area, exceeds the accepted drinking water standard limits (1500 mg/L total dissolved solids) in about half the water-bores tested. An additional constraint is the long-term sustainability of these water resources — especially for the major communities, in which several hundred people have a modern lifestyle and average water consumption is ~500 L/person/day.

The main aquifer types (Fig. 12) are:

- Cainozoic fluvial/lacustrine and alluvial-fan sandy deposits, up to 150 m thick, associated with relict palaeodrainage systems and containing surficial Quaternary calcrete;
  - porous and fractured sandstone and basalt in the Proterozoic–Palaeozoic Amadeus Basin and Ngalia Basin sequences; and
  - fractured igneous and metamorphic rocks of the Arunta Block.
- Most of the area is part of an unconfined to semiconfined elongate groundwater basin draining towards a chain of playa lakes (including Lakes Bennett and Mackay) with a general westerly gradient (Fig. 12).

Recharge has occurred directly through rainwater infiltration to many of the surficial aquifers, and by stream-water infiltration through stream beds. The almost flat potentiometric surface over much of the area suggests that groundwater movement is slow; indeed, groundwater may be locally ponded over an irregular basement topography. Head decay from earlier wetter climatic conditions may also influence the low groundwater gradient.

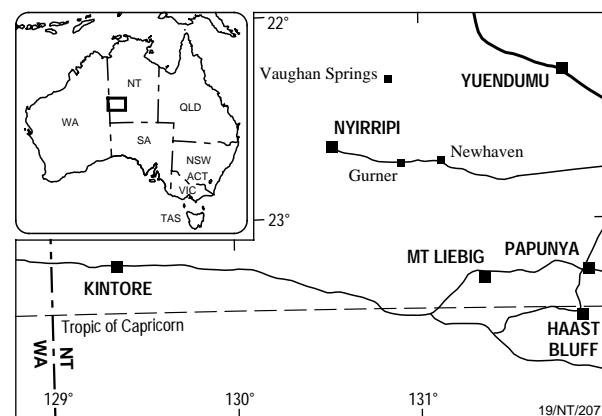


Fig. 11. 'Western water' study location map.

The amount of recharge to the regional aquifers used for the main community water supplies, and therefore the sustainability of these supplies, is questionable. According to hydrographic evidence, a fractured-basalt aquifer at the Kintore settlement receives modern recharge (Wischusen 1994: in 'Papers, water down under', International Association of Hydrogeologists & Institution of Engineers of Australia, Adelaide, 343–349). However, monitoring of water-bores in the fractured-sandstone aquifer at Yuendumu, another large settlement, suggests that only 10 per cent of the extracted groundwater represents recharge — the remainder being 'old' water derived from storage (Berry 1991: Northern Territory Power & Water Authority, Report 07/1991).

In an attempt to elucidate the recharge characteristics, timing, and potential of the area's aquifers, we have integrated data from stable and radioactive ( $^{36}\text{Cl}$  and  $^{14}\text{C}$ ) isotopes with hydrochemical, and hydrogeological data. This contribution focuses on the  $^{36}\text{Cl}$  component of the study.

### The $^{36}\text{Cl}$ technique for dating groundwater

Chlorine-36 is an unstable isotope produced from cosmic-ray interaction in the atmosphere (mainly with argon, and mostly at mid-latitudes) and with near-surface rocks, and by neutron flux arising from radioactive decay of actinides in the subsurface.

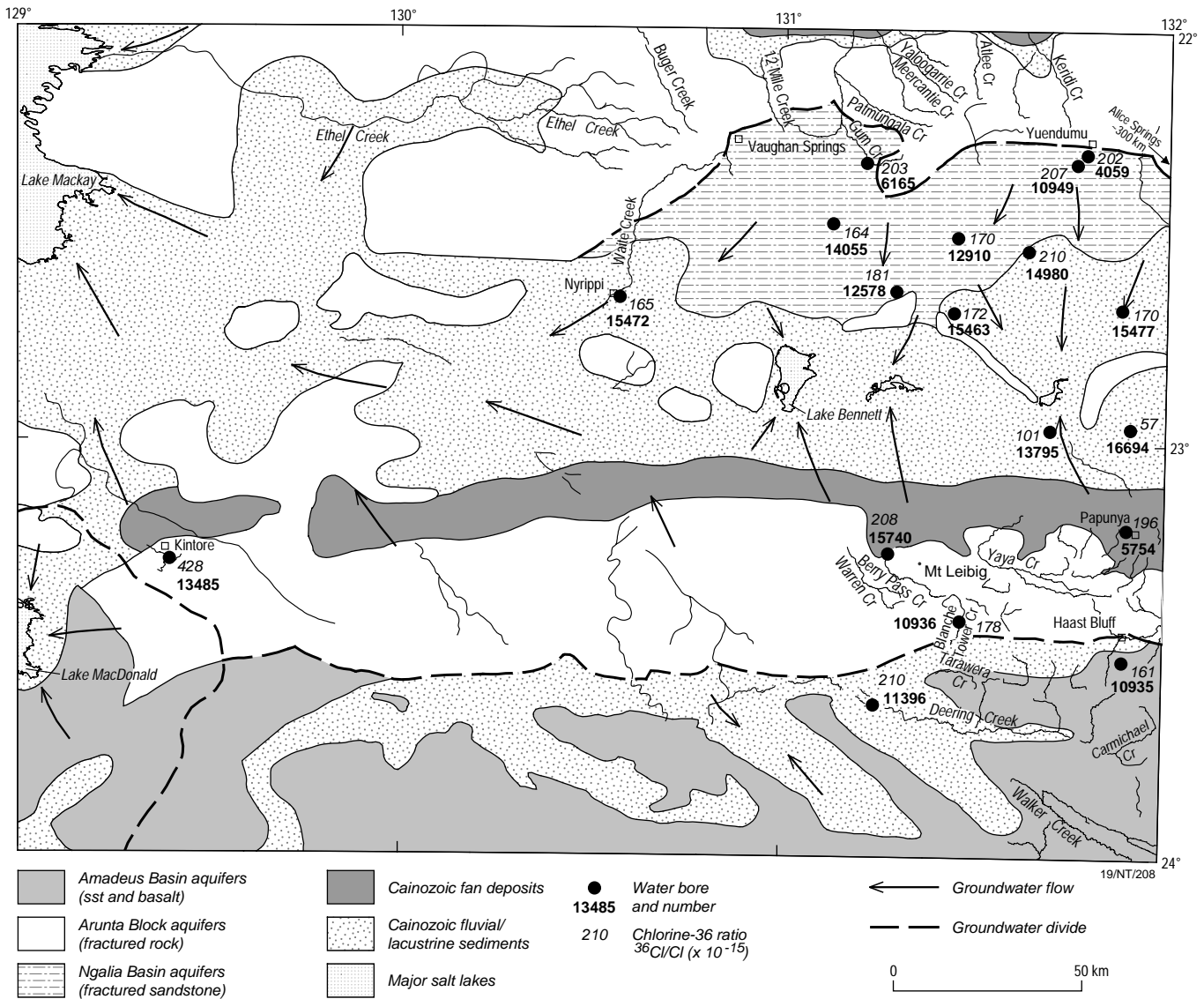


Fig. 12. General hydrogeology, groundwater flow system, bore locations, and major communities in the 'Western water' study.

The atmosphere also contains stable chloride derived from sea-spray and remobilised terrestrial salts. The concentration of this chloride, which diminishes exponentially inland (Keywood et al. 1998: *Journal of Geophysical Research*, 103, 8281–8286), combines with a latitudinal dependence of  $^{36}\text{Cl}$  fallout to give a  $^{36}\text{Cl}/\text{Cl}$  ratio for any given location. This ratio can be measured by accelerator mass spectrometry from a few milligrams of silver chloride precipitated from groundwater, and varies in natural systems from a few hundred parts in  $10^{15}$  of total chloride to a background of a few parts in  $10^{15}$ . Thus, we measure the radioisotope at the attomole level from typically 250 ml of groundwater.

The hydrophilic nature of chloride makes it an ideal conservative tracer in groundwater systems, and the long half-life of  $^{36}\text{Cl}$  (301 000 y) makes it particularly useful in systems with long flow paths. The  $^{36}\text{Cl}/\text{Cl}$  ratio may be used to estimate ages of groundwater if three assumptions are made:

- that the only sink for  $^{36}\text{Cl}$  in the aquifer is radioactive decay;
- that the only source for additional  $^{36}\text{Cl}$  is normal deep subsurface production, or that additional sources can be identified and quantified; and
- that the production rate for  $^{36}\text{Cl}$  is the same now as at the time of recharge.

The groundwater may then be dated from a standard radioactive decay equation.

## Methodology

Eighteen groundwater samples were drawn from shallow aquifers in Cainozoic and Palaeozoic units via operating bores and, to a lesser extent, non-operating bores that were first purged of their standing water (Fig. 12). In addition, three samples were collected from the playa, Lake Ngalia: two surface crusts and one brine collected at a depth of one metre below the crust. For  $^{36}\text{Cl}$  determination, silver chloride was precipitated from each sample by adding silver nitrate at acid pH, and purified to lower the sulphur content. The water content of the precipitate was reduced by drying, and the precipitate was pressed into silver bromide masks in copper holders. Samples of the precipitate were measured in the tandem accelerator at the Australian National University.

## Results and discussion

Spatial variations are apparent in both the geochemical data and  $^{36}\text{Cl}/\text{Cl}$  ratios. Some of them may reflect an irregular subaquifer topography and attendant ponding of old water in localised depressions, as demonstrated for the smaller palaeodrainage system at Uluru (English 1998: 'Cainozoic geology and hydrogeology of Uluru–Kata Tjuta National Park, Northern Territory', AGSO Report). However, most of the  $^{36}\text{Cl}/\text{Cl}$  ratios cluster about two values, which (together with other geochemical data) suggest that two basin-wide events have

affected the  $^{36}\text{Cl}$  contents of the samples.

To investigate the validity of this suggestion, we summed the individual  $^{36}\text{Cl}$  age distributions and performed a Gaussian fit to the resulting data (Fig. 13). The statistical analysis shows that two  $^{36}\text{Cl}/\text{Cl}$  ratios may account for 15 of the 18 data points:  $170 \pm 7 \times 10^{-15}$  and  $205 \pm 7 \times 10^{-15}$ . Among the three other data points, a high-level sample with  $^{36}\text{Cl}/\text{Cl} = 428 \pm 19 \times 10^{-15}$  from the fractured-basalt aquifer at Kintore also exhibits high  $^{14}\text{C}$  (107% modern carbon); this site reveals hydrographic evidence for modern recharge, and the groundwater probably incorporates radionuclides due to bomb-testing. The lowest-level sample, from a Cainozoic aquifer close to the playa chain axis, has a  $^{36}\text{Cl}/\text{Cl}$  ratio of  $57 \pm 5 \times 10^{-15}$ , similar to that measured from the salt crust and brine collected from Lake Ngalia. The third statistically distinct data point has a  $^{36}\text{Cl}/\text{Cl}$  ratio of  $101 \pm 7 \times 10^{-15}$ .

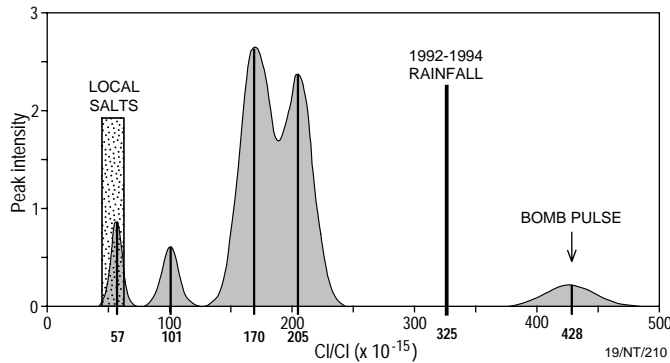


**Fig. 13.** Gaussian distribution of the  $^{36}\text{Cl}/\text{Cl}$  ratio determinations for groundwater samples. Peaks indicate that most of the samples can be accounted for by two distinct ratios.

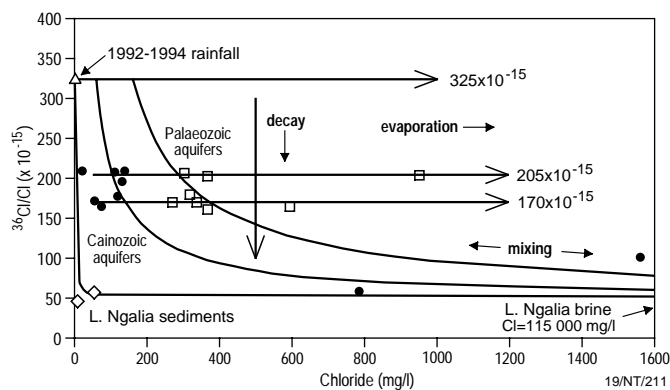


**Fig. 14.**  $^{36}\text{Cl}/\text{Cl}$  ratio versus chloride for groundwater samples. Process trends are indicated by arrows.

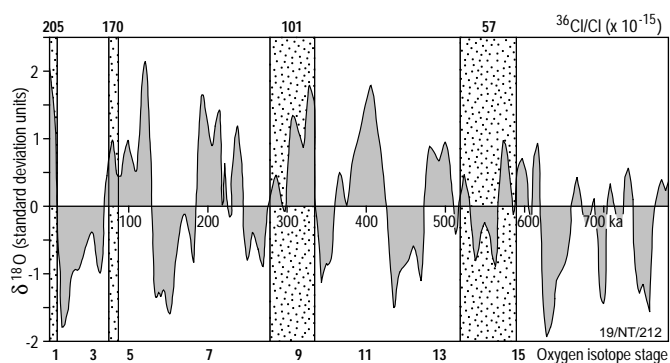


**Fig. 15.** The  $^{36}\text{Cl}/\text{Cl}$  ratios, and their inherent errors, plotted on a time series defined by the SPECMAP  $\delta^{18}\text{O}$  data (Imbrie et al. 1984: op. cit.). High positive  $\delta^{18}\text{O}$  is correlated with global interglacial periods, which were wet in central Australia, and high negative  $\delta^{18}\text{O}$  is correlated with global glacial periods.

On a  $^{36}\text{Cl}/\text{Cl}$  ratio v. chloride plot (Fig. 14; together with lines representing appropriate trends for the processes indicated), the two dominant  $^{36}\text{Cl}/\text{Cl}$  ratios plot as evaporation trends. The distinction between these two trends may be explained in terms of the duration of radioactive decay, and implies that  $^{36}\text{Cl}$  input to the basin occurred during two distinct periods separated by 80 000 y. We infer that  $^{36}\text{Cl}$  input coincided with substantial recharge, which would have happened only during wet climatic regimes.

The higher  $^{36}\text{Cl}/\text{Cl}$  ratio ( $205 \times 10^{-15}$ ) logically records the most recent aquifer recharge. The long half-life of  $^{36}\text{Cl}$ , and the associated analytical errors on the analyses (3%), sanction an interpretation of 'recent' in this sense to be as much as 20 000 y ago. Equally so, the higher  $^{36}\text{Cl}/\text{Cl}$  ratio may represent early Holocene or pre-Holocene recharge water mixed with an insignificant amount of modern water.

Plotting the two ratios on the oxygen-isotope timescale (Imbrie et al. 1984: in Berger et al., 'Milankovitch and climate', NATO, ASI Series, Dordrecht, 269–305) puts the 80 000-y difference between them into perspective (Fig. 15). Wet climatic regimes coincided with interglacial periods. According to geomorphological studies, the wettest period in central Australia over the last full glacial–interglacial cycle, is thought to have been between 80 000 and 110 000 y ago (Kershaw & Nanson 1993: Global and Planetary Change, 7, 1–9). If the  $^{36}\text{Cl}/\text{Cl}$  ratio of  $205 \times 10^{-15}$  records recharge during the current interglacial period, the  $^{36}\text{Cl}/\text{Cl}$  ratio of  $170 \times 10^{-15}$  could represent recharge during the preceding interglacial, and the single-sample ratio of  $101 \times 10^{-15}$  may reflect recharge during an earlier interglacial.

Whereas the main settlement at Kintore appears to be tapping recently recharged groundwater, most of the other settlements are drawing water from a resource that is perhaps 80 000 y or more old. This could have serious implications for the future water security and sustainability of Aboriginal communities across the southwest Northern Territory.

## Conclusions

- The  $^{36}\text{Cl}/\text{Cl}$  ratios of groundwater in shallow aquifers of the southwest Northern Territory cluster in two groups: one, averaging  $205 \times 10^{-15}$ , records recharge probably during the current interglacial period; the other, averaging  $170 \times 10^{-15}$ , may represent recharge during the last interglacial. Without any intermediate values, the two ratios represent recharge separated by a dry interval of 80 000 y.
- The  $^{36}\text{Cl}/\text{Cl}$  ratio of  $428 \times 10^{-15}$  of groundwater representing documented modern recharge in a fractured-basalt aquifer at Kintore probably reflects input of  $^{36}\text{Cl}$  from surface nuclear-bomb testing.
- Low  $^{36}\text{Cl}/\text{Cl}$  ratios observed in some groundwater close to discharge zones probably reflect either dilution by remobilised salt in the subsurface or particularly slow-moving groundwater flow.
- Recharge to the shallow arid-zone aquifers appears to have occurred entirely during wet interglacial periods. This has important implications for groundwater management in this area and elsewhere in central Australia, where many communities rely on groundwater from older (stored) water.

## Acknowledgments

We thank Eleanor Laing for  $^{36}\text{Cl}$  sample preparation. We thank Jim Kellett, Sandy Dodds, Fred Phillips, and John Stuckless for discussion. The project was partly funded by the Aboriginal & Torres Strait Islander Commission.

<sup>1</sup> Geohazards, Land & Water Resources Division, Australian Geological Survey Organisation, GPO Box 378, Canberra, ACT 2601; tel. +61 2 6249 9758 (GJ); fax +61 2 6249 9970 (GJ); email Gerry.Jacobson@agso.gov.au.

<sup>2</sup> Department of Nuclear Physics, Australian National University, Canberra, ACT 0200; tel. +61 2 6249 5179 (RC); fax +61 2 6249 0748 (RC); email richard.cresswell@anu.edu.au.

# Gamma-ray spectrometric and oxygen-isotope mapping of regional alteration halos in massive sulphide districts: an example from Panorama, central Pilbara Craton

David L. Huston<sup>1</sup>, Carl W. Brauhart<sup>2</sup>, Peter Wellman<sup>1</sup>, & Anita S. Andrew<sup>3</sup>

The Panorama district, in the central Pilbara Craton (WA), is perhaps the best exposed, least deformed volcanic-hosted massive sulphide (VHMS) district in the world, and represents an ideal laboratory not only to study the genesis of such deposits but also to test the utility of exploration techniques. Recent studies there indicate that  $\gamma$ -ray spectrometric and whole-rock oxygen-isotope mapping effectively define regional- and local-scale alteration facies in VHMS districts. The application of simple K/Th ratios to  $\gamma$ -ray spectrometric data, acquired as part of AGSO's regional aeromagnetic survey of the Pilbara, defines a regional semiconformable zone of potassium depletion. This zone becomes transgressive below known deposits and prospects. Potassium depletion zones, which were detected remotely, correspond closely with zones of potassium mineral destruction mapped by Brauhart et al. (1998: *Economic Geology*, 93, 292–303). Similarly, oxygen-isotope mapping highlights the same semiconformable and transgressive zones as areas of low  $\delta^{18}\text{O}$ .

Two major (Sulphur Springs and Kangaroo Caves) and a number of smaller Zn–Cu VHMS deposits occur in the Panorama district at

or near the contact between the ca 3.24-Ga Kangaroo Caves Formation and the overlying turbiditic Gorge Creek Group (Fig. 16a). The Kangaroo Caves Formation consists of andesitic to rhyolitic volcanic rocks. It is intruded by the polyphase subvolcanic Strelley Granite, which is inferred to have acted as the heat source driving the hydrothermal circulation that formed the VHMS deposits and associated regional alteration zones.

The volcanic and granitic rocks have been altered into four broad assemblages (Fig. 16b):

- alkali feldspar–chlorite–calcite–quartz–pyrite ('background' spilitic assemblage),
- alkali feldspar–sericite–quartz,
- sericite–quartz, and
- chlorite–quartz.

The chlorite–quartz assemblage is closely associated with ore. It forms a semiconformable zone 0.1–0.2 km thick at the base of the volcanic pile; this zone becomes transgressive immediately below all known prospects (Brauhart et al. 1998: op. cit.).

## Part I. Remote alteration mapping by $\gamma$ -ray spectrometry

David L. Huston<sup>1</sup> & Peter Wellman<sup>1</sup>

As the ore-related alteration assemblage of chlorite–quartz is characterised by a lack of potassium-bearing minerals, this alteration zone should be characterised by low potassium concentrations relative to the surrounding feldspar- and/or sericite-bearing zones. Over the past ten years, the quality of airborne  $\gamma$ -ray spectrometric surveys has improved dramatically, so that the absolute surface concentrations of potassium, uranium, and thorium can be estimated and gridded. Hence, airborne  $\gamma$ -ray spectrometry could effectively map feldspar- and sericite-destructive alteration zones, particularly in well-exposed areas such as the Panorama district.

As part of the joint AGSO–GSWA (Geological Survey of Western Australia) 'North Pilbara' project for the National Geoscience Mapping Accord, AGSO acquired  $\gamma$ -ray spectrometric data over the Panorama district in a 400-m-line-spaced aeromagnetic survey of the central and east Pilbara in mid-1996. A detector-specific calibration facilitated the raw data conversion to compositional data. As mass changes in hydrothermally altered rock are best viewed relative to immobile elements, potassium and uranium concentrations were ratioed to immobile thorium concentrations to produce images showing K/Th and U/Th.

Of these images, that showing K/Th mapped geological variations most effectively (Fig. 16c). Four broad zones with similar K/Th characteristics occur within the Strelley succession:

- a zone of intermediate values (0.14–0.20 % K/ppm Th) in the western (basal) part of the Strelley Granite,
- a zone of low values (0.08–0.14) in the eastern part of the Strelley Granite and the base of the volcanic pile,
- a narrow semiconformable zone of extremely low values (<0.08) in the lower part of the volcanic pile, and
- a zone of higher values (0.14–0.30) at the top of the volcanic pile.

Fingers of low K/Th ratios extend from the narrow semiconformable zone of extremely low values to the Kangaroo Caves and Sulphur Springs deposits (Fig. 16c), as well as the smaller prospects. The overlying Gorge Creek Group is characterised by variable, although generally high K/Th ratios.

Comparison of Figure 16c with Figures 16a and 16b indicates that the K/Th ratio effectively maps not only primary geological features, but also the distribution of important alteration facies within the Panorama district. In particular, the semiconformable zone of extremely low K/Th ratios corresponds closely to the K-mineral deficient zones mapped by Brauhart et al. (1998: op. cit.). The discordant chlorite–quartz feeder zones underlying the VHMS deposits also are characterised by low K/Th ratios. The zone of higher K/Th ratios at the top of the volcanic pile corresponds to feldspar- and sericite-bearing alteration zones.

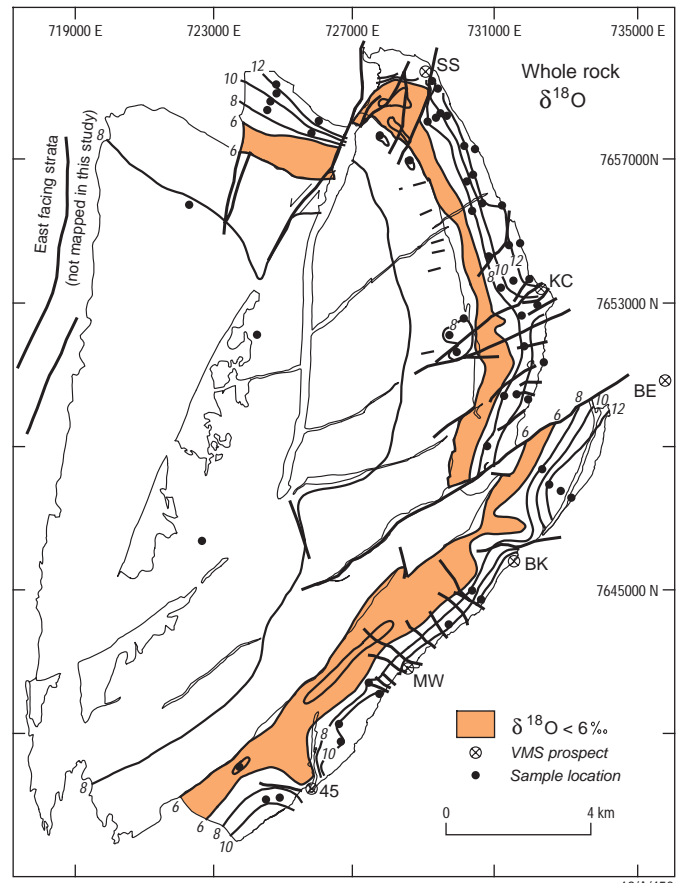
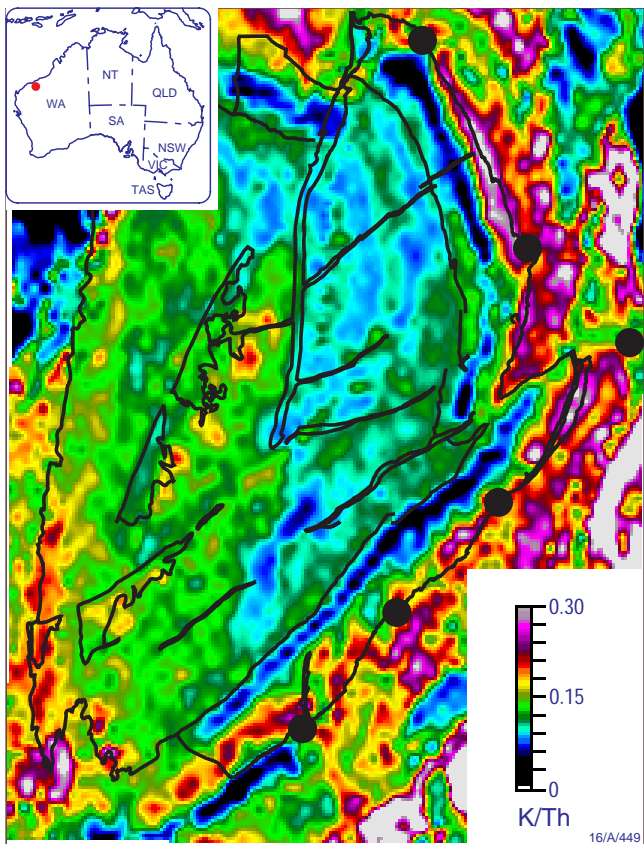
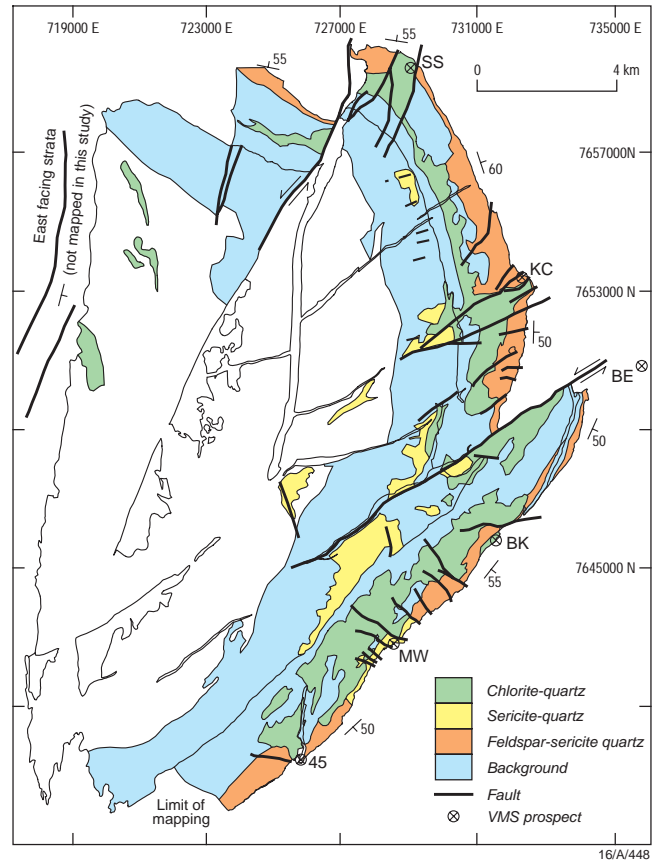
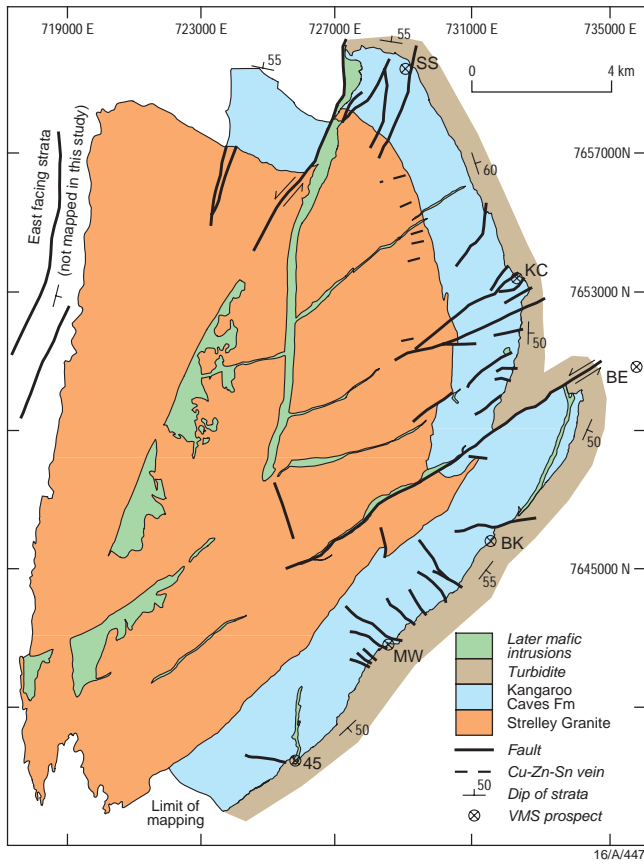


Fig. 16. Maps of the Panorama district showing (a, top left) geology, (b, top right) distribution of alteration facies, (c, bottom left) variations in the K/Th ratio from airborne  $\gamma$ -ray spectrometric data, and (d, bottom right) variations in whole-rock  $\delta^{18}\text{O}$ . Abbreviations of prospect names are as follows: BE = Berndts, BK = Breakers, KC = Kangaroo Caves, MW = Man O'War, SS = Sulphur Springs, and 45 = Anomaly 45 (partly modified after Brauhart et al. 1998: op. cit.).

## Part II. Alteration mapping by oxygen isotopes

Carl W. Brauhart<sup>2</sup>, David L. Huston<sup>1</sup>, & Anita S. Andrew<sup>3</sup>

Although regional studies (e.g., Cathles 1993; Economic Geology, 88, 1483–1511) have demonstrated that the distribution of whole-rock  $\delta^{18}\text{O}$  can define areas of high-temperature fluid flow in VHMS districts, such geochemical studies are not routinely integrated with geological and alteration mapping programs. To investigate the spatial relationship of whole-rock  $\delta^{18}\text{O}$  to alteration facies, 188 fresh samples were analysed for  $\delta^{18}\text{O}$  at the CSIRO Division of Petroleum Resources in Sydney.

Comparing Figures 16d and 16a reveals a steady decrease in  $\delta^{18}\text{O}$  values from 12–14‰ at the top of the volcanic pile to less than 6‰ at the base. Beneath the Sulphur Springs deposit and the Breakers and Anomaly 45 prospects, pronounced discordant low  $\delta^{18}\text{O}$  zones lead up to the mineralised horizon. At Kangaroo Caves and Man O'War, discordant low  $\delta^{18}\text{O}$  zones are not well developed. Within the underlying Strelley Granite,  $\delta^{18}\text{O}$  values are 6–8‰.

According to previous modelling of oxygen-isotope mobility in hydrothermal systems (e.g., Cathles 1993: op. cit.), the dominant control on  $\delta^{18}\text{O}$  distribution (and alteration facies) is the temperature at which hydrothermal fluids alter rocks: whole-rock  $\delta^{18}\text{O}$  decreases with the increasing temperature of fluid-dominated alteration. Hence, the  $\delta^{18}\text{O}$  map shown in Figure 16d can be regarded as a crude map reflecting hydrothermal palaeotemperatures. Consequently, the semiconformable and transgressive low  $\delta^{18}\text{O}$  zones are best interpreted as zones that have undergone intense high-temperature fluid flux. Moreover, zones of very high  $\delta^{18}\text{O}$  are best interpreted as regions that have only reacted at low temperature, without interacting with high-temperature ore fluids. Hence, oxygen-isotope mapping can be used to establish zones of high-temperature and low-temperature fluid flow, information which can be used to focus exploration programs at regional and deposit scales.

### Conclusions

The results of this study indicate that regional alteration facies in VHMS districts can be mapped effectively by remotely sensed  $\gamma$ -ray spectrometric data and by the distribution of whole-rock  $\delta^{18}\text{O}$ . Both techniques may be underutilised by the mineral exploration community. This study indicates that fairly straightforward processing of  $\gamma$ -ray spectrometric data can very effectively delineate regional alteration facies involving potassium metasomatism, particularly in well-exposed terranes such as the Pilbara Craton. Oxygen-isotope mapping effectively defines zones that underwent both low- and high-temperature reaction with hydrothermal fluids; this information can be used in mineral exploration both to focus on zones through which high-temperature ore fluids have passed and to exclude regions that have only interacted with low-temperature fluids.

### Acknowledgments

Sipa Resources and Outokumpu Australia provided partial support for this study. CWB acknowledges the support and interaction with colleagues from the Centre for Teaching and Research in Strategic Mineral Deposits at the University of Western Australia. Andrew Todd is thanked for his assistance in the stable-isotope laboratory. Greg Ewers and Dean Hoatson commented on an early draft of this communication, and Mitch Ratajkoski assisted in the compilation of the diagrams, which Lana Murray prepared for publication.

<sup>1</sup> Minerals Division, Australian Geological Survey Organisation, GPO Box 378, Canberra, ACT 2601; tel. +61 2 6249 9577 (DLH), +61 2 6249 9653 (PW); fax +61 2 6249 9983; email David.Huston@agso.gov.au, Peter.Wellman@agso.gov.au.

<sup>2</sup> Centre for Teaching and Research in Strategic Mineral Deposits, University of Western Australia, Nedlands, WA 6009; tel. +61 8 9481 6259; fax +61 8 9322 3047; email sipa@iinet.com.au.

<sup>3</sup> CSIRO Division of Petroleum Resources, PO Box 136, North Ryde, NSW 1670; tel. +61 2 9490 8743; fax +61 2 9490 8197; email Anita.Andrew@syd.dpr.csiro.au.

## Subeclogitic rocks and their implications for crustal structure in the western Musgrave Block, central Australia

Alastair Stewart<sup>1</sup>

**Subeclogitic rocks — rocks metamorphosed under conditions transitional from granulite to eclogite facies — are known in Australia only in the Musgrave Block (Clarke 1993: AGSO Research Newsletter, 18, 6–7; Clarke et al. 1995a: AGSO Journal of Australian Geology & Geophysics, 16, 127–146; Scrimgeour & Close in press, Journal of Metamorphic Geology; Fig. 17). In the Bates 1:100 000 Sheet area, subeclogitic rocks that formed at ~40-km depth crop out over an area of 2000 km<sup>2</sup>. They are characterised by regionally developed garnet-bearing coronas around mafic grains in Meso- to Neoproterozoic granulite, granite, and mafic dykes. This paper discusses the crustal structure of the western Musgrave Block, and presents two competing schemes for explaining the present crustal structure.**

### Regional setting

The Musgrave Block (Fig. 17) consists of metamorphic rocks, granites (some metamorphosed), layered mafic-ultramafic intrusions (Giles Complex), and mafic dykes. Regional metamorphic facies ranges from greenschist to subeclogite. Major east-striking low to high-angle faults cut the block and penetrate the crust. The largest is the Woodroffe Thrust. North of it, felsic gneisses and deformed granite have amphibolite-facies mineral assemblages dated at 1600–1550 Ma. South of it, felsic and subordinate mafic volcanic and shallow-water sedimentary rocks accumulated between ~1580 and 1300 Ma, and were metamorphosed to granulite facies at about 1200 Ma. Voluminous granite masses dated at about 1190 Ma, outliers of the Giles Complex, and three generations of mafic dykes succeeded the granulites. The relation-

ship of the two regions before they were juxtaposed is not known in the Bates area.

The Woodroffe Thrust dips gently south, and formed during the Petermann Ranges Orogeny at 550–530 Ma in response to north-south compression of the Australian plate (Lambeck & Burgess 1992: Australian Journal of Earth Sciences, 39, 1–19). The Mount Aloysius Fault crosses the Bates area in the south, is steeply south-dipping and normal, and has granulite-facies rocks on both sides. It is inferred from coincident magnetic and topographic lineaments along the northern edge of the Mount Aloysius massif, and from pressure estimates by Clarke et al. (1995a: op. cit.) of 1000–1400 MPa (equating to a depth of formation of 40 km) to the north of the fault and 300–500 MPa to its south.

The subeclogitic rocks, products of regional metamorphism during the Petermann



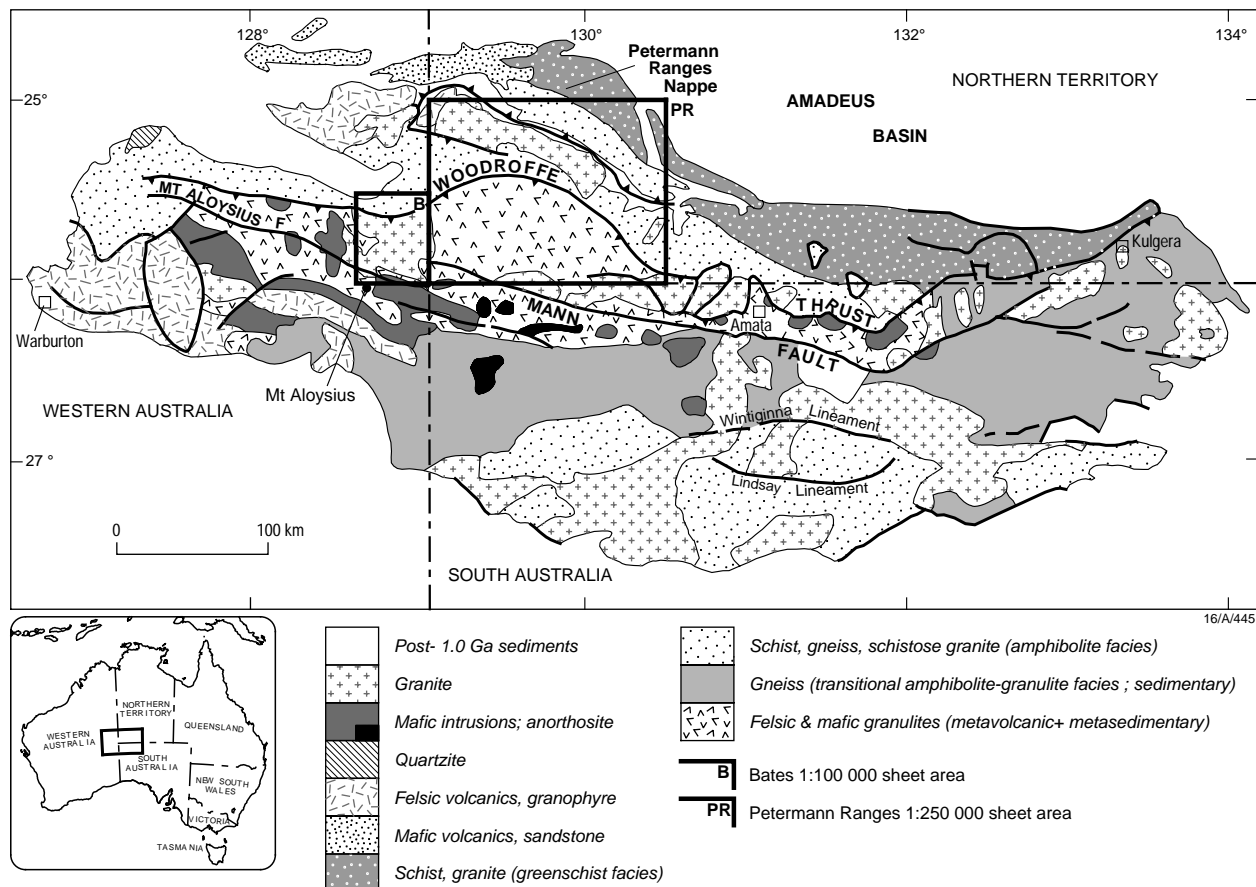


Fig. 17. Simplified geology of the Musgrave Block. The location of the Woodroffe Thrust is from Scrimgeour & Close (in press: op. cit.) in the southwest Northern Territory (cf. D'Addario et al. 1976: *Geology of the Northern Territory*, 1:2 500 000 geological map, Bureau of Mineral Resources/AGSO, Canberra); and from Edgoose et al. (1992: *Kulgera*, 1:250 000 geological map, second edition, Northern Territory Department of Mines & Energy) in the Kulgera area.

Ranges Orogeny, display ubiquitous and spectacular garnet-bearing coronas around mafic grains in the hanging-wall rocks of the Woodroffe Thrust. Mineral assemblages in the intensely deformed thrust zone range from subeclogitic to greenschist, indicating changing metamorphic conditions as the overriding rocks travelled up-dip.

The subeclogitic and other rocks were mapped in detail during 1991 as part of a National Geoscience Mapping Accord investigation of the Giles Complex and its host granulites (Glikson et al. 1996: AGSO Bulletin 239; Stewart 1997: AGSO Record 1997/5).

### Mylonite zones

A mylonite zone 400 m thick in the northern Bates Sheet area delineates the Woodroffe Thrust (Stewart 1995: AGSO Journal of Australian Geology & Geophysics, 16, 147–153), and separates subeclogite-facies metamorphic rocks to the south from deformed granite, from which the mylonite is derived. Similar mylonite (but also containing abundant clasts of garnet derived from metagranite south of the thrust) forms hills tracing a north-northwest-striking tear fault cutting the thrust.

Numerous mylonite zones 1–20 m wide and several hundred metres long cut the subeclogitic rocks south of the Woodroffe Thrust. They comprise subeclogite-facies minerals (White & Clarke 1997: *Journal of Petrology*, 38, 1307–1329). Their sense of shear is dextral, sinistral, reverse, and normal in about equal proportions (at different exposures). Most dip gently to moderately southwards, and have a subhorizontal west-southwest-plunging stretching lineation. These are the same orientations observed in the Woodroffe Thrust, suggesting that the mylonites and thrust are coeval. This is supported by the subeclogite-facies mineral assemblages in the mylonites, which are probably lower-crustal splays of the thrust.

### Granulite-facies metamorphism (1200 Ma)

Where they are unaffected by subeclogitic metamorphism, garnet-bearing assemblages in intermediate and mafic granulites from the area south of Bates have yielded temperature and pressure estimates of 750°C and ~500 MPa for  $D_2$ ,  $D_3$  pressure estimates are 400–600 MPa for a temperature of 700°C (Clarke et al. 1995a: op. cit., p. 130). Gray (1978: *Journal of the Geological Society of*

Australia, 25, 403–414) dated the granulite metamorphism as  $1222 \pm 39$  Ma (Rb–Sr whole-rock isochron), which Sun & Sheraton (1992: AGSO Research Newsletter, 17, 9–10) confirmed with a SHRIMP U–Pb zircon age of 1200 Ma for synmetamorphic augen gneiss.

### Subeclogite-facies metamorphism (535 Ma)

Subeclogite-facies coronas around orthopyroxene, clinopyroxene, hornblende, and opaque grains in rocks south of the Woodroffe Thrust comprise concentric shells of garnet  $\pm$  plagioclase  $\pm$  biotite  $\pm$  clinopyroxene  $\pm$  hornblende  $\pm$  rutile. Pressure estimates are consistently 1000–1400 MPa; temperature estimates range from 700–875°C (Clarke et al. 1995a: op. cit., p. 141; White & Clarke 1997: op. cit.). The subeclogitic metamorphism was dated by Clarke et al. (1995b: AGSO Journal of Australian Geology & Geophysics, 16, 25–39) with Sm–Nd mineral-pair ages of  $536 \pm 16$  and  $533 \pm 16$  Ma for a metagabbro dyke. This agrees with Rb–Sr and Ar–Ar ages of 550–530 Ma for the Petermann Ranges Orogeny 250 km to the east (Maboko et al. 1992: *Australian Journal of Earth Sciences*, 39, 457–471; Camacho & Fanning 1995: *Precambrian Research*, 71, 155–181),

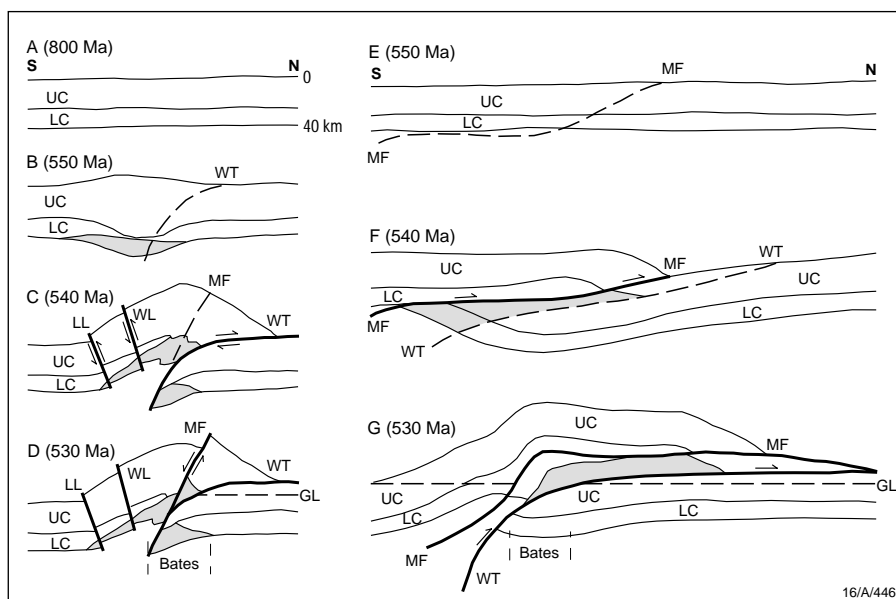


**Fig. 18.** Two diagrammatic cross-sectional models of Neoproterozoic–Cambrian evolution of the western Musgrave Block (and projected locations of the Bates 1:100 000 Sheet area and present ground level, GL; hachuring represents subeclogitic rocks): a–d — after Lambeck & Burgess (1992: op. cit., fig. 11); e–g — after Butler (1986: op. cit., fig. 11). (a) Initial crust (LC, lower crust; UC, upper crust) at 800 Ma. (b) Crustal thickening and position of the Woodroffe Thrust (WT). (c) Overthrusting along the Woodroffe Thrust; reverse faulting along equivalents of the Wintiginna (WL) and Lindsay Lineaments (LL; projected onto the section from the east); and position of the Mann–Mount Aloysius Fault (MF). (d) Normal faulting along the Mann–Mount Aloysius Fault. (e) Initiation of the proto-Mann Fault. (f) Overthrusting along the Mann Fault, and position of the Woodroffe Thrust. (g) Overthrusting along the Woodroffe Thrust and steepening of the Mann Fault.

and with an Sm–Nd garnet–hornblende–whole-rock–mineral isochron age of  $494 \pm 59$  Ma in the adjoining Petermann Ranges 1:250 000 Sheet area (Scrimgeour & Close in press: op. cit.).

### Implications for crustal structure

The present-day crustal structure of the Musgrave Block dates from the Petermann Ranges Orogeny. It has been determined by Lambeck & Burgess (1992: op. cit.) from teleseismic travel-time studies. Overthrusting along the Woodroffe Thrust accounts for the upward movement of the subeclogitic rocks to their present position in Bates, but the mechanism of their descent to 40 km is unclear. Following Lambeck & Burgess, I previously depicted the Woodroffe Thrust as steepening at depth, and invoked underthrusting of the footwall block (Stewart 1997:

op. cit., fig. 17). This left the mid-crustal granulites of the hanging wall stranded above 40 km. Scrimgeour & Close (in press: op. cit.) presented a possible solution when they recognised the regional extent of subeclogitic rocks immediately east of Bates, and concluded that the Petermann Ranges Orogeny involved substantial crustal thickening.

According to one possible sequence of events (Fig. 18a–d), crustal compression and thickening depressed the 1200-Ma-old mid-crustal granulites to subeclogitic-facies depths of 40 km at about 550 Ma (Fig. 18b). East-northeast overthrusting along the Woodroffe Thrust transported the subeclogitic rocks from the lower crust onto upper-crustal amphibolite-facies rocks (Fig. 18c), and accompanied high-angle reverse faulting along equivalents of the Lindsay and Wintiginna Lineaments.

Movement directions on the Mann Fault (Fig. 18d) have long been problematical. Lambeck & Burgess (1992: op. cit., p. 17) considered it to be a thrust. However, their figure 11, which depicts the hanging-wall block above the Woodroffe Thrust as upper crust, conflicts with their textual reference (pp. 11–12) to this block as having a lower-crustal velocity (7.0 km/s). Thus, lower crust south of the Mann Fault is displaced downwards relative to the hanging-wall block of the Woodroffe Thrust — i.e., the nett movement on the Mann Fault was normal. The Mount Aloysius Fault in the south of the Bates region is a splay or *en echelon* offshoot of the Mann Fault to the east. Normal (or transtensional) faulting along the Mount Aloysius–Mann Fault left a crustal wedge as the highest part of the region (Fig. 18d). The subeclogitic lower-crustal rocks in the lower portion of this wedge are preserved as the hanging-wall block of the Woodroffe Thrust in Bates.

An alternative scheme, based on modelling of the Alps and Himalayas (Butler 1986: Journal of the Geological Society of London, 143, 857–873), involves two episodes of thrusting. In Figure 18e–f, underthrusting along the proto-Mann Fault (low-angle) depresses a slab of crust to subeclogitic-facies depths. Subsequent initiation of the Woodroffe Thrust and renewed contraction elevated the subeclogitic rocks to their present level, and steepened the Mann Fault to its present attitude (Fig. 18g).

The two models differ significantly in their sense of movement — normal or reverse — on the Mann Fault, and in their depiction of the Moho just south of the Bates region. The differences could be tested by detailed structural study of the Mann Fault and its adjoining rocks to determine the sense of shear, and by a deep seismic survey across this part of the Musgrave Block.

### Acknowledgments

AGSO colleagues David Blake, Shen-Su Sun, and Peter Wellman reviewed and improved the paper.

<sup>1</sup> Minerals Division, Australian Geological Survey Organisation, GPO Box 378, Canberra, ACT 2601; tel. +61 2 6249 9666; email Alastair.Stewart@agso.gov.au.

## A seismic model of the crust through the Broken Hill Block and Tasman Line

Jim H. Leven<sup>1</sup>, Doug M. Finlayson<sup>1</sup>, Andrew Owen<sup>1</sup>, David Johnstone<sup>1</sup>, & Barry J. Drummond<sup>1</sup>

### Introduction

Wide-angle seismic refraction profiling has helped to resolve crustal structure in the Broken Hill Block and across its eastern-bounding Darling Lineament (part of the

Tasman Line, representing the Late Proterozoic continental rift margin in eastern Australia). The Australian Geodynamics Cooperative Research Centre undertook this work in 1997, primarily to

determine whether the abundant amphibolites in the Broken Hill Block might have been sourced from a mid-crustal magma chamber. A secondary objective was to determine seismic wavespeeds in the

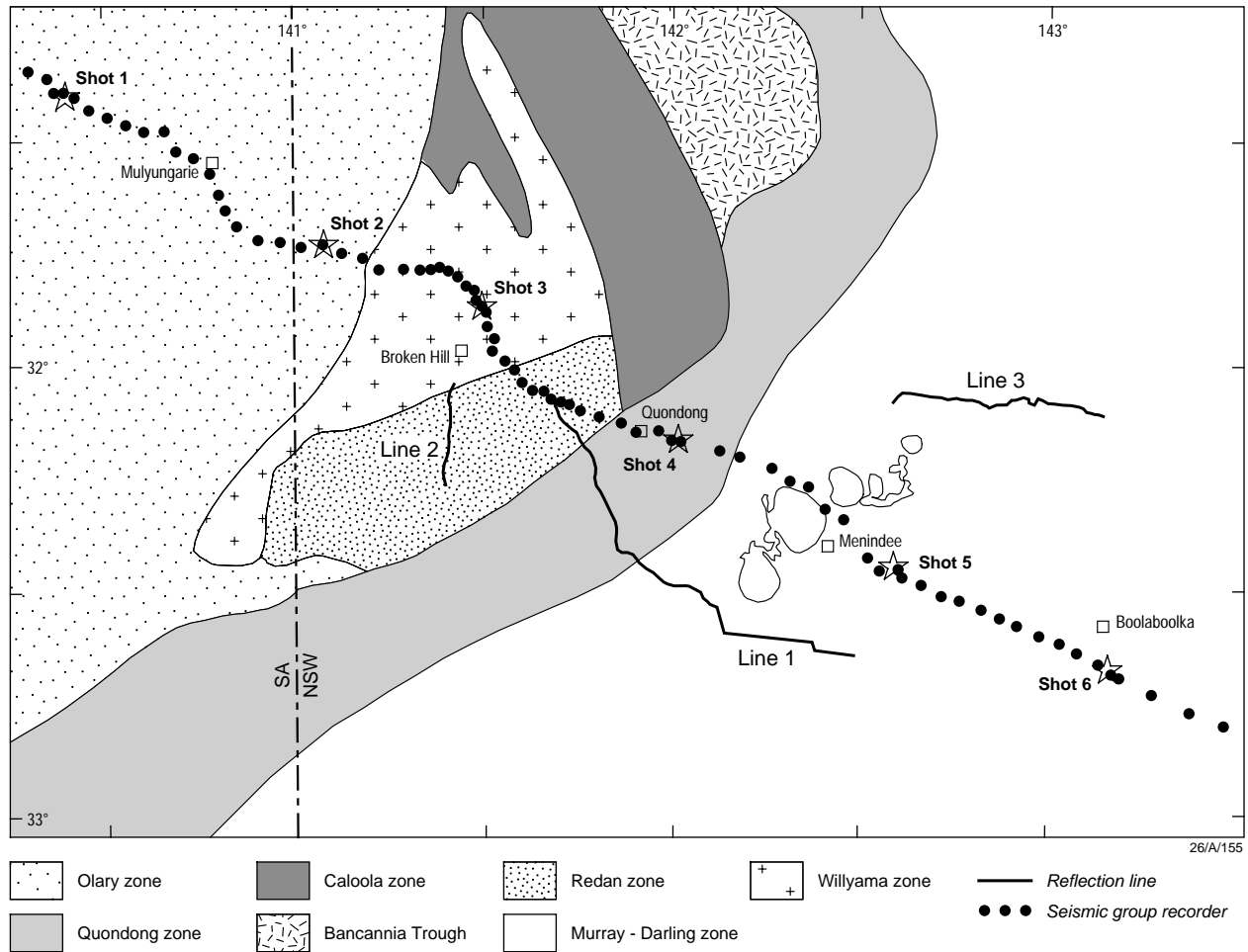


Fig. 19. Location of the Broken Hill wide-angle seismic profile.

crust; lower crust with high wavespeeds is typical in regions with I- (granodiorite) type intrusions, which are common in Proterozoic terranes in Australia but rare in the Broken Hill region.

This work complements AGSO's recent (1996–97) deep seismic reflection profiling through the Broken Hill Block, and represents a further crustal geophysical contribution to the Broken Hill Exploration Initiative for the National Geoscience Mapping Accord. The reflection data show a prominent series of southeast-dipping events, interpreted as shear zones, some extending through the entire crust (Gibson et al. 1998: AGSO Record 1998/11). Within the eastern portion of the Broken Hill Block, the upper crustal shear zones have a listric character and appear to sole into a major detachment at around 10 km depth.

### Wide-angle seismic profiling

Eighty-six seismic group recorders (SGRs) on loan from the United States Geological Survey were deployed along a NW–SE-oriented profile extending over 350 km from the Olary Block (northwest) through the Broken Hill Block to the Murray–Darling Basin (Fig. 19). Station spacing varied from 2.5 km over the Broken Hill Block to 10 km near either end of the profile. Seismic signals were recorded

digitally on tape drives in each instrument during pre-programmed time windows, and shots were fired within these time windows. The seismic signals were detected by 2-Hz geophones buried beside the SGR recorders.

Six shots were detonated during this program. Two 3000-kg shots (1 and 6) were positioned at either end of the profile to provide wide-angle data to offsets in excess of 300 km, and four intermediate, 1000-kg shots (2 to 5) were positioned along the profile to provide additional control on the mid-crustal seismic structure.

### The wide-angle seismic data

The recorded seismic events have been classified into five seismic phases (Fig. 20): Pg1 (upper crustal refracted phase), Pg2 (lower crustal refracted phase), PcP (reflected phase from the mid-crustal boundary), PmP (reflected phase from the Moho), and Pn (Moho headwave phase).

The Pg1 phase for shot 3, detonated north of Broken Hill, has moderately symmetrical travel times about the shot (Fig. 21), and indicates basement P-wavespeed gradually increasing from 5.9 km/s beneath a thin weathering layer. The first arrivals from this shot provide no evidence for a marked variation in P-wavespeed in the upper crust

beneath Broken Hill. In contrast, the Pg1 phase for shot 5 (Fig. 22), detonated near Menindee, evinces a delay-time of 600 ms and prominent asymmetry. Its first arrival times reflect a low-wavespeed near-surface layer, and a large variation in the thickness of this layer and/or upper crustal wavespeed either side of the shot.

Computing the observed arrival times of these various phases has enabled us to construct a P-wavespeed model of the crust along the profile (Fig. 23).

### The model

The model features:

- a two-layer crust:
  - upper layer with P-wavespeeds ranging from 5.9–6.4 km/s; and thickness, 20–30 km (thickest beneath the Broken Hill Block);
  - lower layer with P-wavespeeds ranging from 6.8–7.2 km/s; and moderately constant thickness, around 14 km;
- Moho depth ranges from 35 km on either side to 43 km beneath the Broken Hill Block, and a sub-Moho P-wavespeed of 8.1 km/s;
- low seismic wavespeeds in the upper crust associated with and to the west of the Menindee and Blantyre Troughs, in the

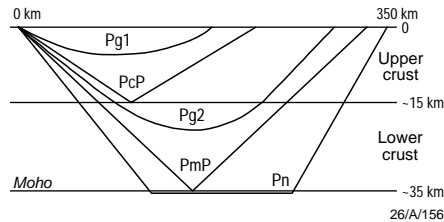


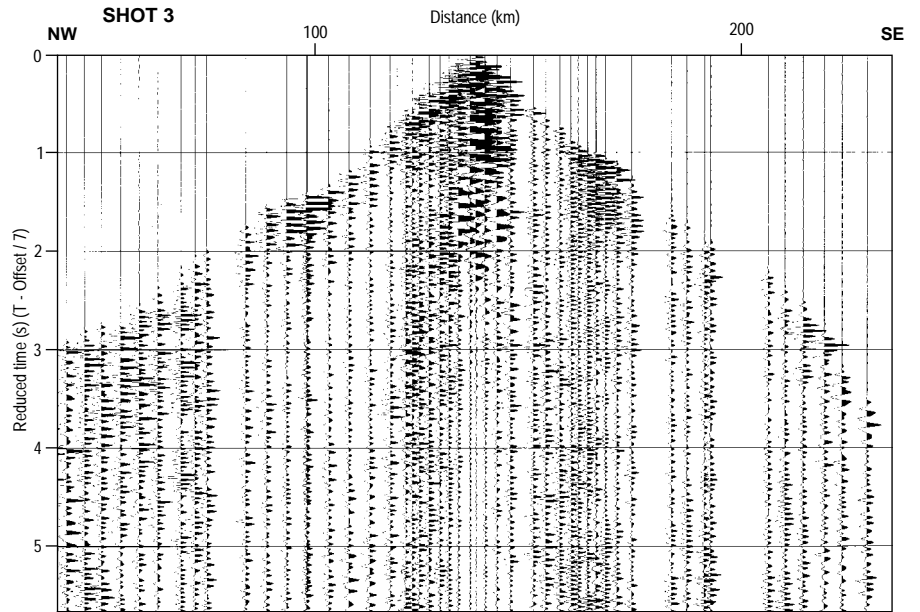
**Fig. 20.** A simplified model showing the major wide-angle (refracted) raypaths.

- region of the Darling Lineament; and
- low lower-crustal P-wavespeeds; no evidence of an underplated lower crustal layer with P-wavespeeds above 7.5 km/s, and therefore no likely source region for I-type (granodiorite) magmas.

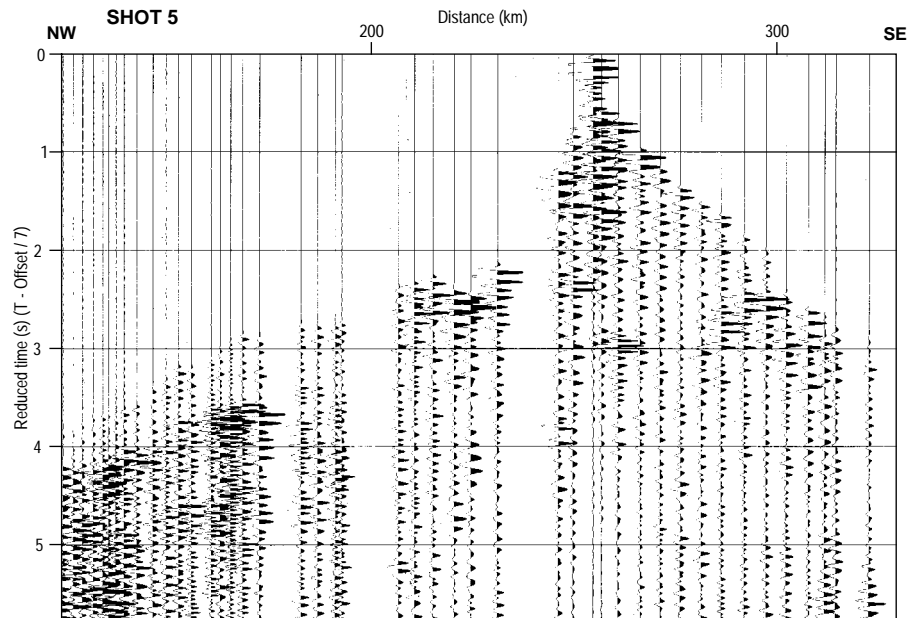
**Conclusions**

The seismic model indicates a prominent thickening of the upper crust beneath Broken Hill, but no associated thickening of the lower crustal layer. Lower crustal P-wavespeeds are lower than world average beneath the Broken Hill Block. A region of low P-wavespeed extends into the basement beneath and to the west of the Menindee Trough.

<sup>1</sup> Australian Geodynamic Cooperative Research Centre (AGCRC) & Australian Geological Survey Organisation, GPO Box 378, Canberra, ACT 2601; tel. +61 2 6249 9275 (JHL); fax +61 2 6249 9972 (JHL); email Jim.Leven@agso.gov.au.



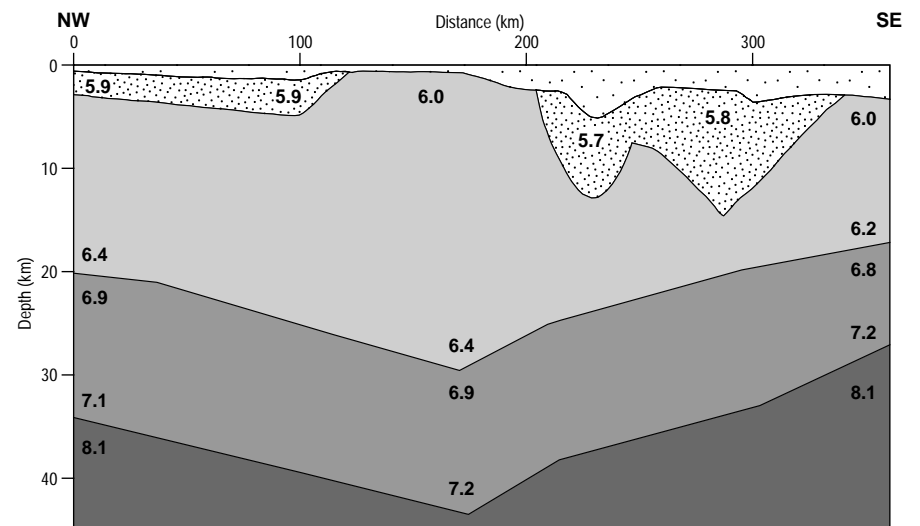
26/A/140



26/A/141

**Fig. 21 (top right).** An example of the Pg1 arrivals from shot 3 detonated north of Broken Hill and recorded across the Broken Hill Block. These Pg1 arrivals show little delay time, indicating the presence of basement rocks with a P-velocity near 5.9 km/s near the surface.

**Fig. 22 (centre right).** An example of the Broken Hill survey Pg1 arrivals from shot 5, detonated east of Menindee. These Pg1 arrivals show a significant delay time, indicating the presence of near-surface low-velocity rocks. The striking asymmetry of the Pg1 arrivals indicates rapidly changing geometry of this low-velocity zone, which corresponds to the Menindee Trough.



26/A/142

**Fig. 23 (lower right).** The P-wavespeed model derived from the seismic arrival times along the Broken Hill profile.

# Structural framework of the northeastern Yilgarn Craton and implications for hydrothermal gold mineralisation

Songfa Liu<sup>1</sup> & She Fa Chen<sup>2</sup>

**The geological history and associated mineralisation of a complex Archaean granite–greenstone terrane can be understood only in the context of its structural evolution. Accordingly, we present a new regional structural synthesis for the northern Eastern Goldfields (Fig. 24) derived from an integration of the results of recent geological mapping with interpretations of aeromagnetic and gravity data\*. This synthesis builds on an earlier one presented for a smaller area (Farrell 1997: in AGSO Record 1997/41, 55–57). It identifies four deformation events (D<sub>1</sub>–D<sub>4</sub>; Table 2), of which two — D<sub>2</sub> (regional ENE–WSW-directed compression) and D<sub>3</sub> (E–W-directed transpression) — largely shaped the region's crustal structure. The structural framework is broadly similar to that documented in the southern Eastern Goldfields (Swager 1997: in AGSO Record 1997/41, 49–53).**

## Deformation history

### First deformation event (D<sub>1</sub>)

The earliest recognisable structures (D<sub>1</sub>) include bedding-parallel foliations, tight to isoclinal folds, and faults. They are evident where they are at high angles (e.g., ENE-trending) to the regional NNW-trending D<sub>2</sub> structures, which commonly overprint them. Elsewhere, they are difficult to distinguish unless overprinting relationships are apparent. Examples of regional D<sub>1</sub> structures include:

- the isoclinal fold refolded by a NNW-trending D<sub>2</sub> antiform at Dingo Range (1);
- bedding-parallel S<sub>1</sub> foliations and associated tight to isoclinal D<sub>1</sub> folds refolded by the D<sub>2</sub> Lawlers Anticline (Platt et al. 1978: Precambrian Research, 7, 3–30);
- several isoclinal D<sub>1</sub> folds refolded by D<sub>3</sub> southwest of Melita (Witt 1994: Melita 1:100 000 geological map explanatory notes, GSWA); and
- the Rio Tinto and Kilkenny synclines [(2) & (3)] and that in the Benalla Hill area (4) recently recognised as D<sub>1</sub> structures by Stewart (this issue, pp. 4–5).

At the southern or northern ends of some granitic domes, an early foliation (S<sub>1</sub>) developed subparallel to the granite–greenstone contact, and was folded during D<sub>2</sub>. Regional D<sub>1</sub> folds apparently are more extensive in the northern Eastern Goldfields than in the south, and so are granite domes.

The exact nature of D<sub>1</sub> is not well understood to date and controversial, but the tight to isoclinal folds reflect compression —

at least locally. According to Hammond & Nisbet (1992: in J.E. Glover (Ed.), 'The Archaean: terrains, processes and metallogeny', Geology Department and University Extension, University of Western Australia, Publication 22, 39–50), their D<sub>E</sub> extensional structures are overprinted by all other deformation events (D<sub>1</sub> to D<sub>3</sub>). They also expressed their inability to distinguish between D<sub>E</sub> tectonic slides, D<sub>1</sub> thrusts in greenstone, and younger D<sub>2</sub> thrusts. Extensional ductile shear zones of low to medium metamorphic grade are also reported in the Leonora area (Skwarnecki 1987: in S.E. Ho & D.I. Groves (Eds.), 'Recent advances in understanding Precambrian gold deposits', Geology Department and University Extension, University of Western Australia, Publication 11, 109–135; Williams & Whitaker 1993: Ore Geology Reviews, 8, 141–162; Passchier 1994: Precambrian Research, 68, 43–64). Hammond & Nisbet (1992: op. cit.) and Williams & Whitaker (1993: op. cit.) suggested north-to-south movement for the early extension, which Passchier (1994: op. cit.) suggested was multidirectional.

We suspect that synvolcanic granite doming during progressive D<sub>1</sub> deformation initiated both extensional shear zones along granite–greenstone contacts, and tight to isoclinal folds between the domes.

### Second deformation event (D<sub>2</sub>)

Regional ENE–WSW-directed shortening during D<sub>2</sub> resulted in the development of prominent NNW-trending folds, faults, and greenstone belts. Regional D<sub>2</sub> folds have wavelengths of 5 to 30 km and are accompanied by penetrative upright axial-planar foliations (S<sub>2</sub>). The deformation intensity is heterogeneous because of rock type differences and deformation partitioning. Overprinting relationships between D<sub>2</sub> structures and D<sub>1</sub> and D<sub>3</sub> structures are locally preserved. For example, near the north shore of Lake Miranda at the southeastern end of an elongate island 3 km south of Bellevue gold mine (5), pillows in metabasalt are markedly flattened and aligned north-northeasterly (parallel to S<sub>1</sub>). The flattened pillows are transected by a prominent N-trending near-vertical cleavage (S<sub>2</sub>) overprinted by D<sub>3</sub> upright folds and S<sub>3</sub> spaced axial-planar crenulation cleavage trending about 330°.

Owing to their style, scale, orientation, and association with granite emplacement, regional D<sub>2</sub> folds and associated S<sub>2</sub> axial-planar foliations can be correlated across the entire northern Eastern Goldfields and with similar structures in the southern Eastern Goldfields. Both provide references for the identification of earlier and later structures where overprinting relationships are preserved.

It is not known, however, if D<sub>1</sub> structures (and similarly for D<sub>3</sub> structures) developed contemporaneously in different areas.

Some D<sub>2</sub> faults and shear zones show evidence of reverse movement. For example, the D<sub>2</sub> Waroonga shear zones (the West Waroonga Shear Zone, Waroonga Shear Zone, and possibly another shear zone between them), up to 5 km wide and more than 100 km long, have an arcuate geometry convex to the east, and coincide with a gravity high (extending east–west across them from greenstone to foliated granitoid) that apparently reflects abundant greenstone below the granitoid. Together, these observations suggest that the shear zones dip to the west. In addition, the West Waroonga Shear Zone is associated with foliations that imply sinistral movement along its northern arm but dextral movement along its southern arm, and dextral movement has been reported along the Waroonga Shear Zone (Platt et al. 1978: op. cit.), which parallels the southern arm of the West Waroonga Shear Zone. These opposing senses of movement indicate eastward differential thrusting. Further, we have interpreted thrust duplexes suggesting westward thrusting along the Eleven Mile Fault (6). The opposing senses of movement along the Waroonga Shear Zone and Eleven Mile Fault probably reflect E–W-directed compression during D<sub>2</sub>.

Reverse movement on D<sub>2</sub> faults generated elongate compressional basins in which the polymictic Jones Creek Conglomerate (7) and Yilgarni Conglomerate (8) were deposited. These conglomerates were deformed in late D<sub>2</sub>, and evince the regional S<sub>2</sub> foliation.

### Third deformation event (D<sub>3</sub>)

E–W-directed transpression during D<sub>3</sub> resulted in the development of regional N- to NE-trending folds, faults, and shear zones. Some N- to NE-trending structures were initiated in D<sub>3</sub>, but others may be reoriented earlier structures. The N- to NE-trending structures developed in D<sub>3</sub> are developed mainly in local compressional areas:

- within newly recognised antidilational jogs defined by NNW-trending sinistral strike-slip faults or lineaments (Chen in press: GSWA Annual Review 1997–98), and
- in wedge-shaped areas defined by N- to NNE-trending and NNW-trending regional faults.

Overprinting relationships between D<sub>3</sub> and earlier structures are locally observed.

The NNE-trending Ockerburry Fault links the zones transected by the NNW-trending Ninnis Fault and Perseverance Fault–Mount George Shear Zone. Several NNE-trending folds with wavelengths of 0.5 to 1 km along the Ockerburry Fault probably developed

\* A contribution to the 'Yilgarn' project, operated jointly by AGSO and the Geological Survey of Western Australia (GSWA) for the National Geoscience Mapping Accord.

during  $D_3$ . The sigmoidal geometry of the Koonoonooka monzogranite east of the Perseverance Fault might have been finally shaped by the  $D_3$  transpressional deformation.

Between the NNE-trending sector of the Mount George Shear Zone and the NW-trending Melita Fault, three major open folds trending NNE to ENE are interpreted as  $D_3$  structures (Witt 1994: *op. cit.*) due to local compression induced by dextral movement along the Mount George Shear Zone and sinistral movement along the Kilkenny and Melita Faults.

In the Kilkenny area, two macroscopic synclines (Rio Tinto (2) and Kilkenny (3)) with wavelengths of 3 to 10 km plunge gently to moderately to the SSW, and are bounded by NNE-trending reverse faults dipping to the east. Chen (*in press: op. cit.*) interprets them as  $D_3$  structures or earlier structures reoriented by  $D_3$  local compression induced by sinistral strike-slip movement along the Kilkenny Fault. Stewart (pp. 4–5, this issue) suggests that they are  $D_1$  folds because an  $S_2$  schistosity cuts the Kilkenny Syncline (3) almost at right-angles.

#### Fourth deformation event ( $D_4$ )

$D_4$  structures are dominated by E-trending normal faults and fractures. Some of the faults displace NNW- to NNE-trending  $D_2$  and  $D_3$  structures, greenstone belts, and gold-bearing veins. Some are filled with mafic/ultramafic dykes of probable Proterozoic age. Kink folds and subhorizontal crenulations, observed in many locations, postdate  $D_3$ , but their relationship with the  $D_4$  faults is not clear.

#### Comments on the timing of lode-gold mineralisation

Most lode-gold deposits in the Yilgarn Craton are structurally controlled and related to metamorphic and/or felsic magmatic fluids. The currently popular continuum model (Groves 1993: *Mineralium Deposita*, 28, 366–374) places the formation of most lode-gold deposits late in the tectonothermal history at 2640–2630 Ma. However, Witt (1997: in AGSO Record 1997/41, 151–156) presented evidence for gold mineralisation other than

**Table 2. Major features of regional deformation events**

|                      |   |
|----------------------|---|
| <b>D<sub>4</sub></b> | East-trending normal faults and fractures   |
| <b>D<sub>3</sub></b> | Regional E–W-directed transpression resulted in N-, NNE- to NE-trending folds, faults, and shear zones mainly within local compressional areas defined by NNW-trending sinistral strike-slip regional faults, and dextral movement along some N- to NNE-trending faults |
| <b>D<sub>2</sub></b> | Regional ENE–WSW-directed compression produced dominant NNW-trending folds, widespread axial-planar foliation, and regional-scale reverse faults associated with deposition of polymictic conglomerates in compressional basins, and emplacement of granitoids          |
| <b>D<sub>1</sub></b> | Tight to isoclinal folds, bedding subparallel foliations and faults, commonly recognised at high angles to regional $D_2$ NNW-trending structures. Intrusion of granitoids comagmatic to late-stages of felsic volcanism  |

that readily explained by the continuum model. Indeed, each of the  $D_1$ – $D_3$  events could have favoured gold mineralisation.

Both heat and fluids for gold mineralisation would have been available when the pre- to syn- $D_1$  granites and their comagmatic felsic volcanics were emplaced. The recently discovered gold deposit at Kanowna Belle, near Kalgoorlie, apparently reflects porphyry-related mineralisation (Ren & Heithersay 1997: *Proceedings of the 9th IAGOD Symposium, Beijing, E. Schweizerbart'sche Verlagsbuchhandlung, Stuttgart, 1–16*); perhaps more are yet to be discovered. Williams et al. (1989: *Australian Journal of Earth Sciences*, 36, 383–403) suggested that gold mineralisation in the Leonora area was associated with  $D_1$ , and so did Harris et al. (1997: *Australian Journal of Earth Sciences*, 44, 503–508) in the Duketon area.

Granite emplacement during  $D_2$  would have generated high temperatures, and fluids aplenty for the intensive regional ENE–WSW-directed shortening to mobilise. Similarly, the regional E–W-directed  $D_3$  transpression should have been a favourable force for mineralisation.

Some mineralised veins evidently predate the cessation of tectonism because they are deformed — e.g., in the Bronzewing area (Phillips et al. 1998: in D.A. Berkman & D.H. Mackenzie (Eds.), 'Geology of Australian and Papua New Guinean mineral deposits', Australasian Institute of Mining & Metallurgy, Melbourne, 127–136; F. Robert, Geological Survey of Canada, personal

communication 1997). Recent work suggests that lode-gold mineralisation at Jundee and Mount McClure occurred before  $2656 \pm 7$  and  $2663 \pm 4$  Ma respectively (Yeats & McNaughton 1997: in AGSO Record 1997/41, 125–130), probably pre- to syn- $D_2$ . Most recently, Bateman et al. (1998: *Geological Society of Australia, Abstracts*, 49, 25) suggested that gold lodes at the Golden Mile in Kalgoorlie were formed during  $D_3$  transpression, and that the mineralising event possibly began during  $D_2$ , rather than previously thought — late in the structural history (~2630 Ma). Perhaps more gold deposits diverse in style and timing, particularly those related to magmatism and to the early structural and metamorphic history, are yet to be identified/discovered.

#### Acknowledgment

This work benefits from discussions with Tim Griffin, Alastair Stewart, Terry Farrell, Steve Wyche, Cees Swager, and Shuangkui Ren. Alastair Stewart and Richard Blewett reviewed and constructively improved the paper. She Fa Chen publishes with the permission of the Director of the Geological Survey of Western Australia.

<sup>1</sup> Minerals Division, Australian Geological Survey Organisation, GPO Box 378, Canberra, ACT 2601; tel. +61 2 6249 9522; fax +61 2 6249 9983; email Songfa.Liu@agso.gov.au.

<sup>2</sup> Kalgoorlie Office, Geological Survey of Western Australia, PO Box 1664, Kalgoorlie, WA 6430; tel. +61 8 9021 9435; fax +61 8 9091 4499; email: s.chen@dme.wa.gov.au.

**Fig. 24 (facing page).** Structural framework of the northeastern Yilgarn Craton compiled from published 1:100 000 and 1:250 000 geological maps and interpretations of aeromagnetic and gravity data. Note that a fold's assignment to  $D_1$ – $D_3$  relates to the deformation event that initiated it (as interpreted by us or compiled from published work cited in the text), and that some early folds may have been reshaped by subsequent deformation.



# Towards national geoscience data standards

Rod Ryburn<sup>1</sup> & Ian O'Donnell<sup>1</sup>

**Geoscience data standards as a field of research may seem like a dull peripheral issue of little relevance to the domain of many geoscientists. However, the subject is gaining rapidly in importance as the information revolution takes hold, because ultimately billions of dollars worth of information are at stake. In this article we take a look at what has happened recently in this field, where we think it is heading, and AGSO's role in establishing national data standards.**

## Petroleum exploration data

The global petroleum exploration and production industry has established a clear lead in the quest for geoscience data standards. About 10 years ago, a contraction of profits in the oil industry forced companies to look carefully at their data-handling efficiency. They found that incompatibilities between software packages and data structures were major inefficiencies. Whereas most professionals were spending ~60 per cent of their time locating, sifting, 'massaging', and transcribing data, many others were being employed just to write programs to transcribe data from one 'stand-alone' system to another.

The magnitude of the industry-wide inefficiencies led to the formation in 1990 of a non-profit organisation — POSC (Petrotechnical Open Software Consortium, see [www.posc.org](http://www.posc.org)), based in the United States and Europe. The original members (BP, Mobil, Elf, Texaco, and Chevron) head a list that has since grown substantially; AGSO, for example, has subscribed for the last 6 years. POSC has established a series of specifications, standards, and logical data models, including both object and relational data models. The POSC data models do not include important geoscience topics, such as biostratigraphy and organic geochemistry, but there are plans to expand their scope. Although these data models are complex, and are fully understood only by the largest companies and petrotechnical software houses, POSC claims that they already result in a saving of US\$1–3 per barrel of oil. This represents a saving of about a billion dollars on the cost of production from the recent oil discoveries on Australia's North West Shelf.

Another similar consortium to which AGSO subscribes is PPDM (Public Petroleum Data Model Association, see [www.ppdm.org](http://www.ppdm.org)), based in Calgary, Canada. PPDM's data models are more concrete than POSC's big-picture logical models, but the two organisations are not in competition.

## Mineral exploration data

The mineral exploration industry lags a long way behind the example set by its petroleum counterpart. Nevertheless, some steps have been taken to formulate mineral data standards. For years, GGIPAC (Government Geoscience Information Policy Advisory Committee; formerly GGDPAC), which advises the Australian Chief Government Geologists (CGG), has been grappling with the problem, particularly the standards for reporting mineral exploration data to State governments. The problem is tripartite:

- **Legacy data.** 'Hard-copy' exploration reports, maps, and sections submitted to State mines departments must be captured as electronic bit-images, and appropriate metadata and storage facilities established so that the images can be distributed online. The Department of Mineral Resources (NSW) has shown the way here via its successful DIGS ('Digital imaging geological survey system') project (see [www.slnsw.gov.au/ILANET/clients/mineral\\_resources/about/gsgenerl.htm#digs](http://www.slnsw.gov.au/ILANET/clients/mineral_resources/about/gsgenerl.htm#digs)), which has invested millions of dollars electronically capturing over two billion dollars worth of exploration data.
- **Future reports.** The next step is to ensure that future reports are submitted in computer-readable form for text-searchable online access. The initial recommendation to GGDPAC that SGML (Standard Graphics Markup Language) be used (see draft guidelines at [www.dme.nt.gov.au/library/ggdpac96.html#INTR](http://www.dme.nt.gov.au/library/ggdpac96.html#INTR))

was rejected by NSW. A possible solution is to allow exploration companies to submit reports as word-processed documents suitable for translation to PDF format for web viewing. The State authorities would still need to maintain a proper metadata base of reports, and large maps, etc., would require scanning as images.

- **Hard data.** The greatest difficulty is maximising the usefulness of all the hard data consigned to maps, tables, and diagrams in exploration reports and their appendices — i.e., the valuable data concerned with sample locations, drillholes, core logs, lithologies, chemical analyses, geophysical surveys and many other aspects of mineral exploration. To this end, these data must be placed in a proper information management system — i.e., a standardised database system — and submitted in this way by the exploration companies. Simpler schemes, such as spreadsheets and ASCII files, can never provide the required degree of standardisation and data integrity. Unfortunately, an agreed standard database system to match this requirement does not yet exist.

## The AMIRA geoscience data model

As long ago as 1992, State mines departments, via GGDPAC, recognised that standard geoscience data models were needed across the mineral exploration industry, and arranged for AMIRA (Australian Mineral Industries Research Association, see [www.amira.com.au](http://www.amira.com.au)) to manage project P431 — 'The geoscience data model'. The Australasian Spatial Data Exchange Centre was contracted to formulate a data model. Major sponsors were the State governments and AGSO. Disappointingly, only two industry sponsors, BHP Exploration and North Exploration, came forward. The themes that were included in the model were geology, drilling, geochemistry, and mineral resource/reserve.

The model, which was delivered in April 1998, reflects a great deal of consultation, including input canvassed from existing database models. It consists of entity-relationship diagrams (cf. Fig. 25) and a data dictionary for the agreed themes. Several practicality tests were applied to it, including a Microsoft Access database covering the Broken Hill region constructed from data supplied by government agencies. These were successful, and proved the feasibility of transferring existing databases to the new model.

The project has since been criticised for not delivering a working solution to the problem of company data submission. This was never on the agenda, and is a far more complex task that requires a much higher order of commitment — probably several million dollars worth, in terms of software development. At the same time, the AMIRA model, useful as it already is, needs to be expanded to cover a wider range of geoscience data.

## Where to now?

For mineral exploration data standards to advance, resources must first be pooled — as in the oil industry under POSC. The importance of such a pooling of resources was acknowledged at the 'Gold round table' conference, held in Canberra in February 1998. In a joint paper prepared for submission to the Australia & New Zealand Mineral Exploration Council in July 1988, the Western Australian Mines Department and the CGG Conference estimated that about \$50 million would be needed from the States and Commonwealth to capture electronically the \$30 billion of exploration data held in Australia. If each State attempts to 'go it alone', the ultimate cost will be far higher, and the opportunity to standardise will be lost. With its excellent system of reporting exploration results to government, Australia should lead the world in setting geoscience data standards. We stand to reap rich rewards if we can solve this issue. The technical aspects are not difficult. However, industry (as opposed to government) needs to be much more involved in these issues than it presently is.

Notwithstanding their government-reporting obligations, the mineral exploration industry would benefit from the adoption of



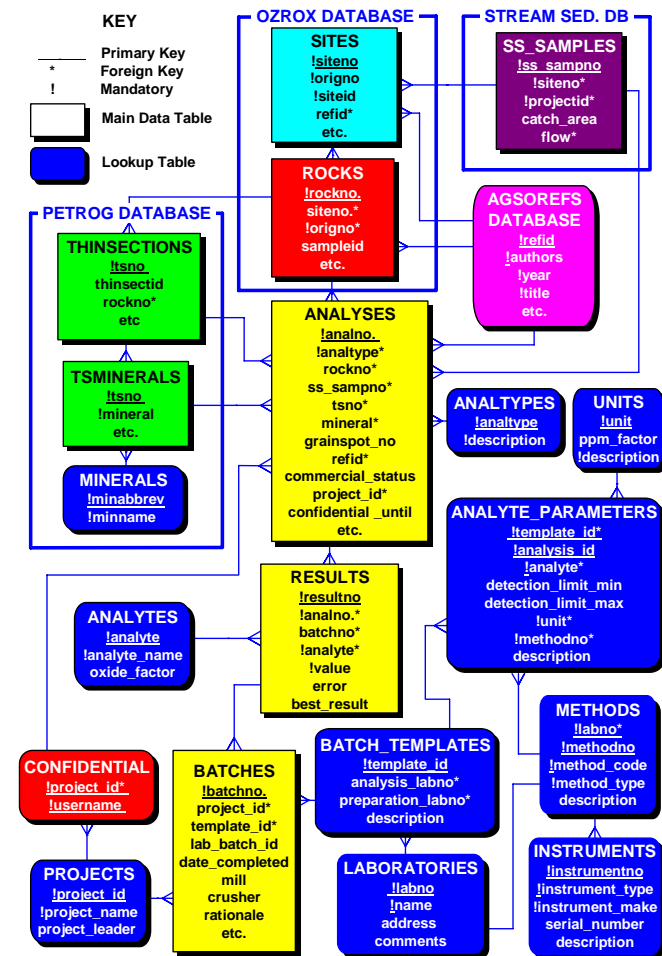


Fig. 25. A table-relationship diagram of the OZCHEM database together with the relevant parts of related databases. The rounded boxes are lookup tables. 'Crows feet' indicate multiple end-of-one-to-many table linkages.

standard data models and software by eliminating the time wasted by employees dealing with non-standard data — an inefficiency probably of a similar magnitude to that reported by the 'pre-standards' oil industry. No one company or government organisation can solve this problem on its own. We have to cooperate to compete!

### AGSO's role in data standards

Although AGSO has no statutory role in collecting mineral exploration data, it has responsibility for national geoscience datasets. Through its Spatial Information & Mapping Services, AGSO takes a keen interest in all national geoscience standards, and maintains many national standard databases and authority tables. The 'National stratigraphic names' database (see [www.agso.gov.au/information/structure/isd/database/stratnames.html](http://www.agso.gov.au/information/structure/isd/database/stratnames.html)) is an example of a standards database, while our geological timescale (GEOTIME) is representative of our numerous authority tables (see [www.agso.gov.au/information/structure/isd/database/lookups.html](http://www.agso.gov.au/information/structure/isd/database/lookups.html)). Most of our standard databases and lookup tables are now visible on our worldwide web site ([www.agso.gov.au](http://www.agso.gov.au)). The development of classification schemes and 'domains' (lists of all possible values an attribute can assume) are as much a part of national standards as are the logical data models and data dictionaries.

In addition to promoting geoscience data standardisation for the benefit of petroleum and mineral exploration, AGSO also addresses data standards for land management, marine science, the environment, and geohazards. Our recently compiled GWATER database is an

example of our attempts to adopt AGSO standards in groundwater and water quality, and AGSO and the States are currently involved in a major effort to define national standards there. Databases that AGSO has compiled for earthquakes, landslides, and tsunamis represent the beginnings of national geohazards data standards. We also support metadata standards, the most important being the Australia New Zealand Land Information Council spatial metadata standard.

### The impact of good data models

The impact of good data models is best explained with an example from AGSO's stable. For many years, AGSO maintained several diverse laboratory analytical databases typically consisting of wide tables corresponding to various analytical instruments and techniques. Thus, trace-element geochemistry was recorded in over 60 columns, one for each element, and organic geochemistry had over 700 different columns for each analyte. For every newly added method or analyte, new columns had to be added to the tables, or even whole new tables built. We recently restructured some of these databases into the OZCHEM database (Fig. 25).

OZCHEM is a fully 'normalised' database in which a long 'skinny' table called RESULTS substitutes for several previous 'fat' tables. For each sample analysed, RESULTS has many rows — usually one for each element or analyte processed. The identity of each analyte, the numerical analytical result, and pointers to other tables with errors, methods, unit, etc., are entered in RESULTS. This structure allows for multiple determinations of the one analyte by various laboratories. Also, any number of new analytes and methods can be added without having to change the database's structure. With the help of the latest database software, OZCHEM performs well, and attractive user interfaces are easily built.

OZCHEM can now manage whole-rock chemistry, stream-sediment geochemistry, and microprobe analyses of minerals and rocks. In theory it could be made to handle isotopes, organic geochemistry, and water chemistry as well — a universal geochemical database — but we have not integrated all these disparate analytical disciplines (and maintain separate analytical databases for groundwater and organic geochemistry).

From a corporate perspective, the efficiencies to be gained by pooling all analytical results in the one generalised, analytical database are spectacular, and an example of how good generalised database models can save a lot of time and effort.

### Conclusions

- The global petroleum exploration industry has shown the way to uniform data standards by pooling resources in their POSDC and PPDM non-profit organisations.
- The mineral exploration industry needs to do the same. It must cooperate to compete.
- Australia is in a good position to lead the world in mineral exploration data standards, but both industry and government need to be involved.
- Australian States must standardise their mineral exploration reporting requirements.
- AGSO has a strong role in promoting national geoscience data standards.
- Good data models save time and money. They establish the *lingua franca* of geoscience.

### Acknowledgments

Thanks to Murray Hazell for the diagram of the OZCHEM database, and to John Bradshaw, Murray Hazell, and Frank Brassil for reviewing the manuscript.

<sup>1</sup> Spatial Information & Mapping Services, Science & Survey Support Division, Australian Geological Survey Organisation, PO Box 378, Canberra, ACT 2601; tel. +61 2 6249 9605 (RR), +61 2 6249 9100 (IO); fax +61 2 6249 9942 (RR), +61 2 6249 9984 (IO); email Rod.Ryburn@agso.gov.au, Ian.Odonnell@agso.gov.au.

# Metallogenic potential of the felsic igneous rocks of the Tennant Creek and Davenport Provinces, Northern Territory

Is the enigma of the source of the gold at Tennant Creek resolved?

Lesley Wyborn<sup>1</sup>, Anthony Budd<sup>1</sup>, & Irina Bastrakova<sup>1</sup>

**A review of metallogenic potential suggests that the Au deposits in the Tennant Creek district (NT) are likely to be associated with the ~1820-Ma granites/felsic volcanics of the Treasure Suite, which is prominently exposed in the Davenport Province southeast of Tennant Creek. The ~1850-Ma Tennant Creek Supersuite, which comprises the main granite bodies exposed in the Tennant Creek Province, is a generally unfractionated, restite-rich supersuite older than the Au deposits, and probably had no direct role in ore formation, although its emplacement may have enhanced the formation of the ironstones which host most of the ore. Although the ~1710-Ma Devils Suite evolved a major late fluid phase and is associated with extensive alteration of both the granites and the surrounding country rocks, it had no association with Au mineralisation, and its potential is believed to be limited by the high F content of the parent magma.**

The origin of Au–Cu–Bi deposits in the Palaeoproterozoic Tennant Creek district has inspired debate for over 70 years. Magmatic sources of metals and fluids have been an integral part of many models for the genesis of the deposits. However, age determinations have proved enigmatic, as the spatially nearest granites to the Tennant Creek goldfield appear to be at least 20 m.y. older than accepted ages for the mineralisation (Black 1977: *BMR Journal of Australian Geology & Geophysics*, 2, 111–122; Black 1984: *Australian Journal of Earth Sciences*, 31, 123–131; Compston & McDougall 1994: *Precambrian Research*, 71, 107–129; Compston & McDougall 1995: *Australian Journal of Earth Sciences*, 41, 609–616).

Two major and distinctive regional hydrothermal alteration events in the Tennant Creek Province may have contributed to the mineralisation process. During the first, ironstone hosts of the main Au deposits precipitated from basinal brines (Wedekind et al. 1989: *Economic Geology*, Monograph, 6, 168–

179; Zaw et al. 1994: *AusIMM Publication Series 5/94*, 185–188) in dilational sites early during the regional deformation paragenesis (Ding & Giles 1993: *Proceedings of the International Symposium on Gold Mining Technology*, Beijing, 100). Hydrogen- and oxygen-isotope data imply that a magmatic fluid was unlikely to have been involved in the production of the ironstones (Wedekind 1989: 'Workshop Manual 3', June 1989, University of Tasmania, 45–55).

The second hydrothermal event occurred late in the deformation history (Ding & Giles 1993: *op. cit.*), and has been dated at 1830–1825 Ma by Ar–Ar techniques (Compston & McDougall 1994: *op. cit.*) and 1820–1805 Ma by Rb–Sr methods (Black 1977: *op. cit.*).

The sources of the metals and fluids during mineralisation have been extensively debated, and a magmatic input was postulated (Wedekind et al. 1989: *op. cit.*; Zhaw et al. 1994: *op. cit.*). If magmas were directly involved, the question may be asked: Which one of the three main magma suites in the Tennant Creek/Davenport Provinces sourced the mineralisation?

## The ~1850-Ma Tennant Creek Supersuite

The components of the Tennant Creek Supersuite include the Tennant Creek Granite, Mumbilla Granodiorite, Cabbage Gum Granite, Hill of Leaders Granite, Channinggum Granite, the Epenarra and Warrego Volcanics, and various porphyries and volcanics of the Bernborough and Warramunga Formations (Donnellan et al. 1995: 'Flynn 5759, Tennant Creek 5758', Northern Territory Geological Survey, 1:100 000 Geological Map Series explanatory notes; Blake et al. 1987: *BMR/AGSO Bulletin* 226). Ages range from 1872–1837 Ma, and young progressively southeastwards (Black 1984: *op. cit.*). The supersuite is an I-(granodiorite) type and mainly unfractionated, although there is evidence of weak fractionation in the more felsic end members.

The Tennant Creek Supersuite has

minimal mineral potential. It is associated with minor W mineralisation in the southeast, in the Mosquito Creek tungsten field (Fig. 26), where it is weakly fractionated. Although it appears to have no direct relationship to the Au–Cu–Bi deposits, it may have provided a heat source to enhance the circulation of the basinal brines that formed their ironstone hosts.

## The ~1820-Ma Treasure Suite

The Treasure Suite is composed mainly of volcanics, and shallow intrusive granophyres and porphyries of the Wundirgi Formation, Treasure Volcanics, Arabulja Volcanics, and Newlands Volcanics in the Davenport Province; and unnamed diorites to monzodiorites, and felsic to intermediate volcanics of the Hayward Creek Formation of the Tomkinson Creek Subgroup, in the Tennant Creek Province (Blake et al. 1987: *op. cit.*; Donnellan et al. 1995: *op. cit.*). The suite, a fractionated I-(granodiorite) type, has its more mafic end-members preserved in the northwest Tennant Creek area, and more felsic fractionated members in the southeast, where volcanics and granophyres are more heavily concentrated.

The members of this suite range in age from 1829–1816 Ma (Blake & Page 1988: *Precambrian Research*, 40/41, 329–340). These ages are roughly equivalent to the Ar–Ar ages of muscovite formed during Au–Cu–Bi mineralisation at Tennant Creek — that is, 1830–1825 Ma (Compston & McDougall 1994: *op. cit.*).

The bulk of the Tennant Creek Au deposits coincide with a prominent gravity low (Fig. 26). Granite modelled underneath the Tennant Creek Au field (Rattenbury 1994: *Mineralium Deposita*, 29, 301–308) may be a pluton of the Treasure Suite, whose measured rock densities (2.63–2.68 t/m<sup>3</sup> with a mean of 2.65 t/m<sup>3</sup>; Hone in Blake et al. 1987: *op. cit.*) are compatible with the gravity model. In contrast, the measured densities of Tennant Creek Supersuite rocks (2.68–2.74 t/m<sup>3</sup> with a mean of 2.71 t/m<sup>3</sup>; Hone in Blake et al. 1987: *op. cit.*) are too high.

With regard to **mineral potential**, the Treasure Suite is clearly related to the Hatches Creek tungsten field. Dunnet & Harding's (1967: BMR Report 114) suggestion that the mafic diorites of the suite can be linked to the Au mineralisation at Tennant Creek is borne out by their similar (emplacement and mineralisation) ages. In addition, the total metal budget in the two deposit types is similar: the Hatches Creek W deposits contain Cu, Co, Bi, Mo, and minor U and Sn; and the associated elements in the Au deposits at Tennant Creek are Cu, Bi, Mo, Se, Pb, Co, and minor W and Sn (Large 1974: *Economic Geology*, 70, 1387–1413; Ferenczi 1994: AusIMM Publication Series, 5/94, 171–177). Perhaps the dominance of W in the Davenport Province reflects the more felsic compositions and the predominance of extrusive volcanics in the southeast. The Treasure Suite is also of a similar age to the major Au-related magmatic events farther north and west, in the Pine Creek and Tanami Provinces.

### The ~1710-Ma Devils Suite

The Devils Suite is an extremely fractionated, oxidised, fluorite-bearing I- (granodiorite) type associated with minor vein-W deposits. Comprising the Devils Marbles, Elkedra, and Warrego Granites, it has a high but limited SiO<sub>2</sub> content, and shows abundant evidence of late magmatic–hydrothermal alteration, both within the granite and for some distance into the surrounding country rocks. The related thermal event has also caused considerable isotopic disturbance of the ore deposits in the northwestern part of the Tennant Creek Province (Black 1977: *op. cit.*; Compston & McDougall 1995: *op. cit.*). Despite Wedekind & Love's (1990: AusIMM, Monograph 14, 839–843) demonstration that the Warrego Granite has contact-metamorphosed the Warrego Au–Cu–Bi deposit, Stoltz & Morrison (1994: *Mineralium Deposita*, 29, 261–274) considered this granite to

be genetically related to the Warrego deposit.

Although this suite attests to late magmatic fluid release, the presence of fluorite is believed to downgrade its **mineral potential**, and it probably has only limited potential for vein W. Even though cassiterite is ubiquitous in stream sediments (Hoatson & Cruikshank 1985: BMR Record 1985/44), and alluvial Sn has been extracted from watercourses draining the Wauchope tungsten field (P. Ferenczi, NTGS, written communication 1997), the Devils Suite is highly oxidised; consequently, the Sn probably occurs as cassiterite disseminated throughout its source granite, rather than in late veins.

### Conclusions and future work

We consider that the Au mineralisation was associated with the emplacement of the ~1820-Ma Treasure Suite. The major, ironstone-hosted Au–Cu–Bi deposits occur in the Tennant Creek Province only, presumably because ironstones are poorly developed in the Davenport Province (Blake et al. 1987: *op. cit.*). However, minor quartz-vein Au deposits occur in younger, mainly arenite-rich units and mafic and felsic intrusives/extrusives in both provinces (P. Ferenczi, NTGS, written communication 1997). Similar but larger deposits (cf. the Mount Todd Au deposit at Pine Creek) perhaps await discovery. If so, they will not be located by the magnetic-based exploration techniques which have been applied successfully to target the ironstone-hosted deposits.

For those espousing the view that Au is remobilised by magmatic fluids from country rock (rather than being sourced by granite), the Devils Suite offers food for thought. This suite provides abundant evidence for the release of a late magmatic fluid and attendant alteration of the surrounding country rock; even so, this alteration has clearly not remobilised any Au from the surrounding area. In contrast, the Au mineralisation appears to

be related to an earlier suite that did not as pervasively alter the country rocks surrounding the intrusions.

In the Tennant Creek Province, much effort has been expended in applying geochemistry to distinguish between barren and mineralised ironstones. Even when 'prospective' ironstones are identified, the evidence of Au mineralisation presents a small and difficult target. A more effective methodology may be to investigate the alteration and geochemistry of the porphyries, granites, and quartzofeldspathic rocks surrounding the ironstones (and indeed away from the ironstones) as a means of determining the mineralisation-related fluid pathways.

Future work in the Tennant Creek Province should focus on tapping into the wealth of alteration data in the AGSO ROCKCHEM dataset, to try to delineate vectors to ore in the quartzofeldspathic sequences. Many of the members of the Tennant Creek Supersuite have either a Na- or K-alteration overprint, whereas the younger suites have a K overprint only. Huston & Cozens (1994: *Mineralium Deposita*, 29, 275–287) recorded a mineralised post-ironstone porphyry with K-alteration geochemistry similar to that documented in the AGSO dataset.

### Acknowledgments

This paper results from the joint AGSO/State/Territory 'Metallogenic potential of Australian Proterozoic granites' project, sponsored by 20 companies. It was compiled with considerable assistance from Dave Blake, Dean Hoatson, Dave Huston, Roger Skirrow (AGSO), Nigel Donnellan, and Phil Ferenczi (NTGS). Reviews by Roger Skirrow and Terry Mernagh are gratefully acknowledged.

<sup>1</sup> Minerals Division, Australian Geological Survey Organisation, GPO Box 378, Canberra, ACT 2601; tel. +61 2 6249 9489 (LW), +61 2 6249 9574 (AB), +61 2 6249 9201 (IB), fax +61 2 6249 9971; email Lesley.Wyborn@agso.gov.au, Anthony.Budd@agso.gov.au, Irina.Bastrakova@agso.gov.au.

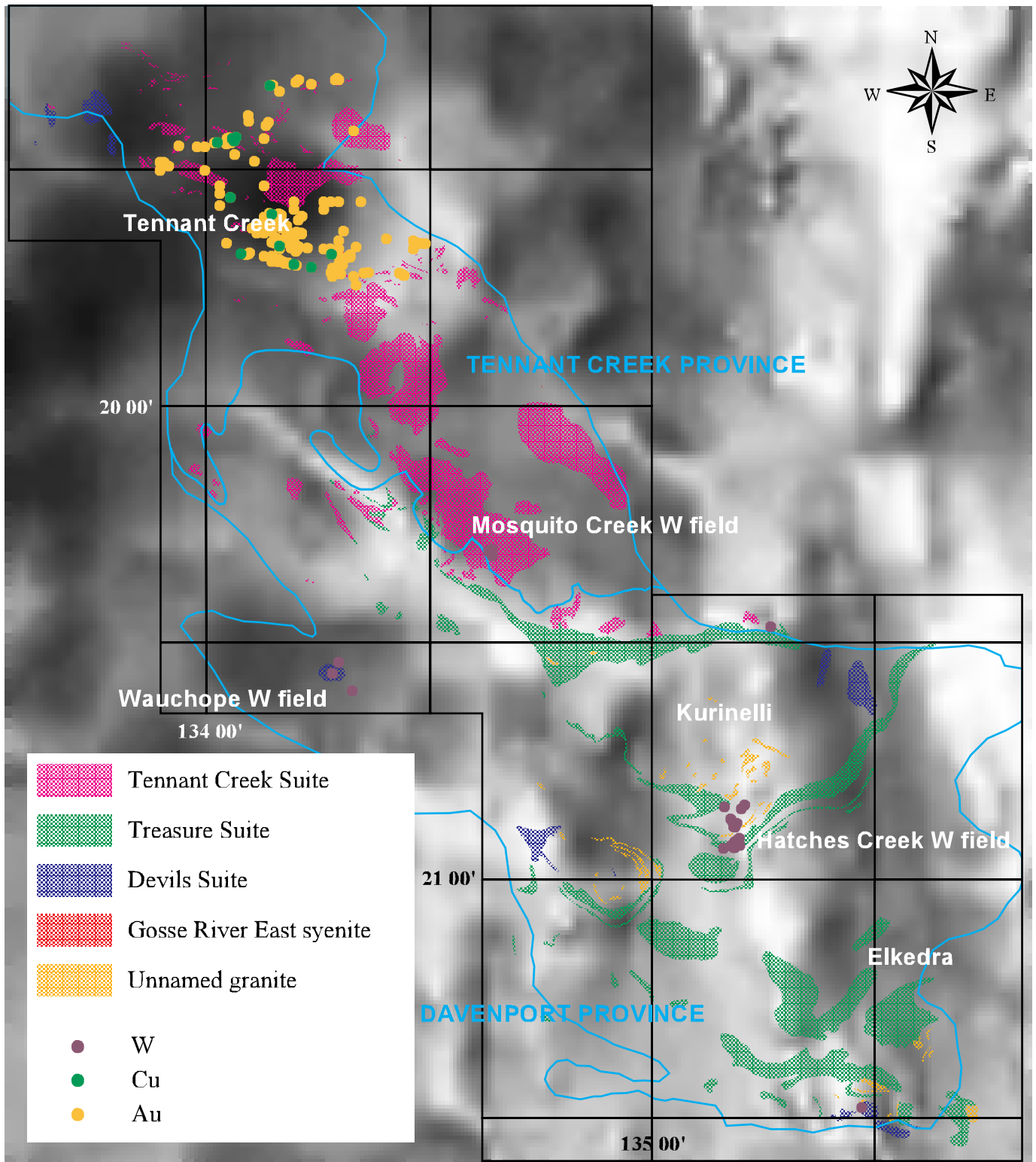


Fig. 26. Distribution of the various granite suites of the Tennant Creek/Davenport Provinces overlain on an image prepared from AGSO's 'Australian national gravity' database. Mineral deposit locations and commodities are from the AGSO/BRS MINLOC database. Note that the Gosse River syenite appears as a small outcrop in the southeast Tennant Creek Sheet area, and is represented by the tiny speck 2–3 mm below the 'A' of 'TENNANT CREEK PROVINCE'.